Politecnico di Torino

Master in Mechanical Engineering – LM-33(DM270)

Thesis Title

Numerical Simulation of Steel Heat treatments

Thesis Supervisor

PROF. PAOLO MATTEIS
Politecnico Di Torino

Candidate

Salman Sakandar
S246599

ABSTRACT

The main aim of this thesis is to simulate solid state metallurgical processes like quenching and tempering in steels. The thesis consists of two parts. In the first part steel hardenability by end quenching test (JOMINY test) was simulated and in the second part Time quenching (self-tempering) was done. The steel used for the first part of experiment is C45 which is medium carbon steel with carbon content of about 0.45% and for second part AISI 1020 is used which is 0.17% carbon steel.

Jominy test is used to check hardenability of steel using a standard specimen of diameter 25 mm and length 100 mm. The specimen is heated at around 900 [deg C] and then quenched at one end using water. The duration of test is about 3200 seconds. In this simulation all the phases are detected and plotted against time. Finally, hardness of steel is calculated. Due to quenching with water at one end of specimen almost all the austenite is transformed into martensite due to extremely high value of heat coefficient. On top of martensite there is a small portion where bainite is dominant while everywhere else its pearlite. Hardness is calculated at different distances from quenched end using phase fraction values for each phase and then multiply it with the hardness value of that phase. Finally, these values were added to get total hardness at that point.

In the quenching and self-tempering phase, a specimen of 32 mm diameter is heated to around 950 [deg C] and then initially quenched using water until surface temperature becomes less than starting temperature of martensite. Then the specimen was left for slow cooling in the air. Since the core is at higher temperature heat is transferred to the surface and increase in surface temperature is observed. This cause self-tempering of steel. The method is useful in making steel rebars which are used for reinforced concrete construction.

Finally in order to test the precision of software results were compared with those given in literature. Also, the final hardness values were compared to experimentally determined values for same steel obtained through literature. Results were comparable to experimental values and trends were same.

ACKNOWLEDGEMENT

First and foremost, I want to convey my heartfelt appreciation to Professor Paolo Matteis at Politecnico Di Torino, who served as a teacher, mentor, and lead supervisor during this work. None of this work would have been possible without his unwavering patience, direction, and inspiration. He has undoubtedly contributed to my growth as an individual and as a researcher providing me with an outstanding example of professionalism and intelligence.

Additionally, I must show my appreciation for various faculty and staff at the Politecnico Di Torino, particularly those in the Mechanical Engineering department, for the invaluable lessons in my major subjects, which helped me make this thesis possible. Also, all the professors from my bachelor's degree, especially Professor Zaib Shahid, deserve recognition for consistently guiding me toward my goals and serving as the true motivation that a young student desperately needs.

Finally, I would like to dedicate this work to my parents, who have always believed in me, to achieve my goals - all my friends and family for their support through thick and thin.

Salman Sakandar

TABLE OF CONTENTS

LIST OF TABLES

LIST OF FIGURES

LIST OF ACRONYMS

TTT	Time Temperature Transformation
K	Thermal Conductivity
C_p	Specific heat at constant pressure
K	Thermal conductivity
$\Delta H_{s\rightarrow d}$	Latent heat of phase transformation
C	Carbon
Si	Silicon
Mn	Manganese
V	Vanadium
Cr	Chromium
P	Phosphorus
S	Sulphur
Cu	Copper
Ni	Nickel

1 Literature Review

The application of Finite Element Method dates to mid of 20th century. During 1950s and 1960 a lot of work was being to solve differential equation using FEM. Several countries had used common method which was to join many small elements to create a mesh structure which was used to discretize continuous complex domain. Finite element simulations predict microstructure and properties of steels. These predictions can be significantly improved by different models proposed in literature. In our case austenite decomposition kinetics were modelled using famous JMAK and Koistinen-Marburger equations. JMAK equation is used to calculate phase fraction as a function of time under isothermal conditions. In most cases austenite decomposition is not isothermal so the principle of additivity proposed by scheil[15] and further developed by Avrami[15] can be used.

With the progress being made in the field of technology and extremely powerful computers available in market a lot of companies developed extremely useful software's which could run these simulations in very less time. One Such software is COMSOL which is used in this thesis. The reason to use this software is that its complete, easy to use, accurate and has wide applications in academic as well as industrial field. Another advantage of using COMSOL is that it has built in model for JMAK, Leblond and Koistinen-Marburger equations. During this thesis two simulation relating to quenching and tempering of steel will be focused and both of these simulations were performed using these built-in models. This software is not limited to these models as it provides option for user defined model where different equations can be added.

First one being very famous test to check hardenability of steel known as Jominy test or End Quench Test. In this test a standard specimen is heated until all of it becomes austenite and then quenched at one end using water at room temperature. While other sides are cooled by convection in air. Then hardness is calculated at several distances from quenched end of specimen.

Second one is time quenching and self-tempering of steel. Also, in this test completely austenitic steel is quenched using water for few seconds and then left in air to be cooled. Due to high core temperature, the temperature at surface rises which cause self-tempering phenomenon. This is very useful process as it has many applications, most famous of them being Rebars. Steel bars once hot rolled are sprayed with water which quenches outer surface of bar and reduces surface temperature. Since the core is at higher temperature than the surface, these two try to balance each other hence raising surface temperature. This causes self-tempering of bar.

1.1 Quenching and Tempering:

Quenching is rapid cooling process of heated specimen to achieve desired phase and hence the desired properties. In metallurgy the most common application of quenching is to increase hardness of steel by inducing martensite. The process includes heating of steel specimen until it becomes completely austenitic and then rapidly cooled using oil or water, this causes austenite to become martensite hence increasing hardness of specimen. Often hardening of steel makes it brittle due to excessive martensite so another heat treatment known as tempering is used.

Tempering is a heat-treating procedure that improves the toughness of iron-based alloys. Tempering is done after hardening to reduce part of the excess hardness, and it involves heating the metal to a temperature below the critical point for a length of time, then cooling it in still air. The amount of hardness reduced is determined by the exact temperature, which is dependent on both the alloy's composition and the desired qualities in the completed product.

The Combination of quenching and tempering give very good mechanical properties which are at a balance, Hardness is lower than that achieved only by quenching, but ductility is a bit more. So mostly combination of both these heat treatments is very common in metallurgy.

1.2 Thermal aspects:

Thermal treatments will be applied to the material, causing major changes at the microscopic and, as a result, macroscopic levels. The equation used to examine this phenomenon is the same as the one used to represent heat conduction, and it goes like this:

$$cp(\partial T/\partial t) = \nabla \cdot (k\nabla T) \qquad \text{……..Equation 1}$$

Equation 1 is applied to inner volume of specimen. where cp stands for heat capacity at constant pressure and k stands for thermal conductivity, are the material's attributes. Another equation is used to describe the thermal exchange during the cooling process. It's known as the convective heat flux formula, and it's written as:

$$q_0 = h \cdot (T_{met} - T_{fluid}) \qquad \text{……Equation 2}$$

Equation 2 is applied to the surface of specimen. Here q_0 is heat flux, h is heat transfer coefficient and T is temperature for fluid and material. This equation is used for heat transfer by convection or phase transition. Heat flux is flow of energy from specimen to fluid per unit area per unit time. Its unit is watt per meter square.

1.3 Metallurgical aspects

1.3.1 Phase Transformation

Steel can exist in different phases depending on temperature and cooling rate. These phases we are dealing with are as follows:

- **Pearlite:**

  It is a mixture and cementite and ferrite with two phased layered structure known as lamellae.

- **Bainite:**

  Similar to pearlite in terms of composition but has different internal structure. Cementite is present in small components in ferrite.

- **Martensite:**

  Formed due to trapped carbon atoms when structure change from FCC austenite to BCC ferrite due to extreme cooling rate. This phase guarantees highest hardness, but it is very brittle.

1.4 Phase Transformation Models

Different type of phase transformation models can be used for our simulations depending on our requirements. Here few models will be briefly explained.

1.4.1 Leblond-Devaux model

As it is expected from the name, this phase transformation model is based on the work of Leblond and Devaux[11], it was presented in 1984. phase transformations based on carbon diffusion are focused on in this model. These transformations are austenite to ferrite and austenite to bainite. Leblond- Devaux model has two forms

- General coefficients
- Time and equilibrium

1.4.1.1 General coefficients

In this form the transition of source phase (s) into destination phase (d) is given by following equation

$$\dot{\xi}^{d} = K_{s \to d}\xi^{s} - L_{s \to d}\xi^{d}$$

Equation 3

For phase transformation to be active, right-hand size of this equation needs to be strictly positive. In general functions K and L depend on temperature. In case of bainite transformation these function K and L depends on cooling rate alongside temperature.

1.4.1.2 Time and equilibrium

This is special form of General coefficient. Here an equilibrium phase fraction for destination phase and a time constant are used to define phase transformation. Is is given by following equation

$$\dot{\xi}^{d} = \frac{\xi_{eq}^{d} - \xi^{d}}{\tau_{s \to d}}$$

Equation 4

For a phase transformation to occur, right side needs to be positive. Here both destination phase and time constant are dependent on temperature.

1.4.2 The Johnson-Mehl-Avrami-kolmogorov (JMAK) model

This model is generalization of Leblond-Devaux model. It is based on Avrami equation which was derived in 1937 by Kolmogorov and was used by Avrami in series of articles published in Journals of Chemical physics between 1939 and 1941.

$$\xi^d = \xi^d_{eq}\left(1 - exp\left(-\left(\frac{t}{\tau_{s\to d}}\right)^{n_{s\to d}}\right)\right)$$

Equation 5

The equilibrium phase fraction $\xi^d{}_{eq}$, time constant τ and avrami constant n are all dependent on temperature. This equation can be expressed in the differential form as follows

$$\dot{\xi}^d = \left(\xi^d_{eq} - \xi^d\right)\frac{n_{s\to d}}{\tau_{s\to d}}\left(-\ln\left(1 - \frac{\xi^d}{\xi^d_{eq}}\right)\right)^{1-1/n_{s\to d}}$$

Equation 6

In this form explicit time dependence is removed. ξ^d which is destination phase needs to be positive for phase transformation to occur. In special case where n which is Avrami constant becomes equal to one, this equation reduced to Time and Equilibrium form of Leblond-Devaux model. The differential form has a mathematical disadvantage as initial destination phase equal to zero will yield 0 trivial solution, as log will evaluate to zero. There are two ways to fix this problem, first one is to put small but finite value of initial destination phase and second is to modify equation so that it does not yield trivial solution.

1.4.3 The Koistinen-Marburger model

This model was developed by Koistinen and Marburger[12] in 1959. It is used to model austenite to martensite transformation which are diffusion less in iron-carbon alloys and carbon steels. The transformation is characterized by critical temperature also known as martensite start temperature M_s. Above this temperature no transformation occurs between austenite and martensite. Koistinen-Marburger equation can be written as follows

$$\dot{\xi}^d = -\xi^s \beta \dot{T}$$

Equation 7

Here β is Koistinen-Marburger coefficient. The transformation from austenite to martensite only occurs below M_s and only during cooling phase. In order to make transformation numerically smooth a parameter ΔMs is used. This makes the transformation gradual. Its value should be chosen small enough so that the start temperature characteristic is retained.

1.4.4 Li model

JMAK equation was enabled by Scheil's principle of additivity and further improved by Avrami to be used in non-isothermal conditions. Cahn[13] proved that isothermal equations like JMAK can be used for calculation of transformation in non-isothermal conditions, by using additive rule. Lusk and Jou[14] proved that in order to apply rule of additivity for phase transformation restrictive conditions exist.

Li[9] modified the transformation model presented by Kirkaldy and Venugopalan (1984) and presented his work in in 1998. Both these models consist of two functions, g(V) which is an integrated function showing microconstituent volume fraction and f(T) which takes into account the effect of temperature and chemical composition on transformation.

$$\frac{dV}{dt} = K(T)^{1/n} \cdot n \cdot (1-V) \cdot \left(\ln \frac{1}{1-V}\right)^{(n-1)/n} = f(T) \cdot g(V)$$

Equation 8

V is the volume fraction of final phase, T is temperature and t is time. k and n are constants derived from experimental data; they show rate of transformation. The additive rule is valid for this equation as f(T) is time dependant and g(V) depends on volume fraction. The integrated function R(V) determines start and finish of transformation and rate of transformation. R(V) is independent of chemical composition and transformation temperature. The integrated forms proposed by Kirkaldy (R_k) and Li (R_L) were modified using phase transformation diagrams to obtain

$$R_K(V) = \int_0^V \frac{dV}{V^{2(1-V)/3}(1-V)^{2V/3}}$$

$$R_L(V) = \int_0^V \frac{dV}{V^{0.4(1-V)}(1-V)^{0.4V}}$$

Equation 9

There are many models developed by researchers to study and characterize solid state transformation. Some famous models are developed by Umemoto[17], Agarwal[18], Suehiro[19], Lee[20] and Lee[21]. The mathematical model presented by Homberg was based on Scheil's additivity rule and Johnson-Mehl equations. For rapid metallurgical heat treatment, Le mason[23] developed a numerical model to estimate two dimensional convection heat transfer coefficient. Umemoto[17] combined isothermal transformation kinetics of pearlite with additivity rule and derived an expression for continuous cooling transformation of pearlite. Using this equation for corresponding TTT diagram, he calculated ideal critical diameter, Jominy distance, Hardness values and critical cooling rates with good accuracy. Suehiro[19] developed a mathematical model for phase transformation prediction of hypoeutectoid steels during continuous cooling. He used small numbers of experimental parameters so that the model can be used on wide range of chemical compositions and temperatures. Lee[20] modelled TTT diagram using nucleation theory with fitted constants. As a function on nucleation energy and activation energy, transformation start C-curves were represented on diagram. He used JMAK equations for increase in volume fraction with time. By using this method he was able to estimate large number of TTT diagrams for steels with different chemical composition. Lee[21] developed a model used to simulate temperature, deformation and phase transformation for both thickness and width of a strip on runout table in hot strip mill. He used continuous cooling experiments to derive phase transformation kinetics.

1.5 Experimental data Jominy test

In order to compare the accuracy of our simulation as well as that of software, we need experimental model to compare our results with. Luckily there is lot of work done on Jominy test and I was able to find a lot of data on the topic. One such work is done by Nunura and Santos[7], they performed Jominy test on three austenitizing temperatures at 800 ℃, 850 ℃ and 900 ℃. To obtain cooling curves at different points thermocouples were placed at predefined positions. Standardized specimen of 25.4 mm diameter and 100 mm length was heated to austenitizing temperature and then cooled at one end with water to produce martensitic formation. Hardness was measured from quenched end along intervals of 1.6 mm. Initial values came highest as expected due to formation of martensite. The value of hardness keeps on decreasing as we move away form quenched end due to low values of martensite. Similar work was done by Homberg[22] who showed numerical algorithm to simulate Jominy test and derived cooling diagrams for AISI 1080 steel. The cooling curves plotted are shown in Figure 2.

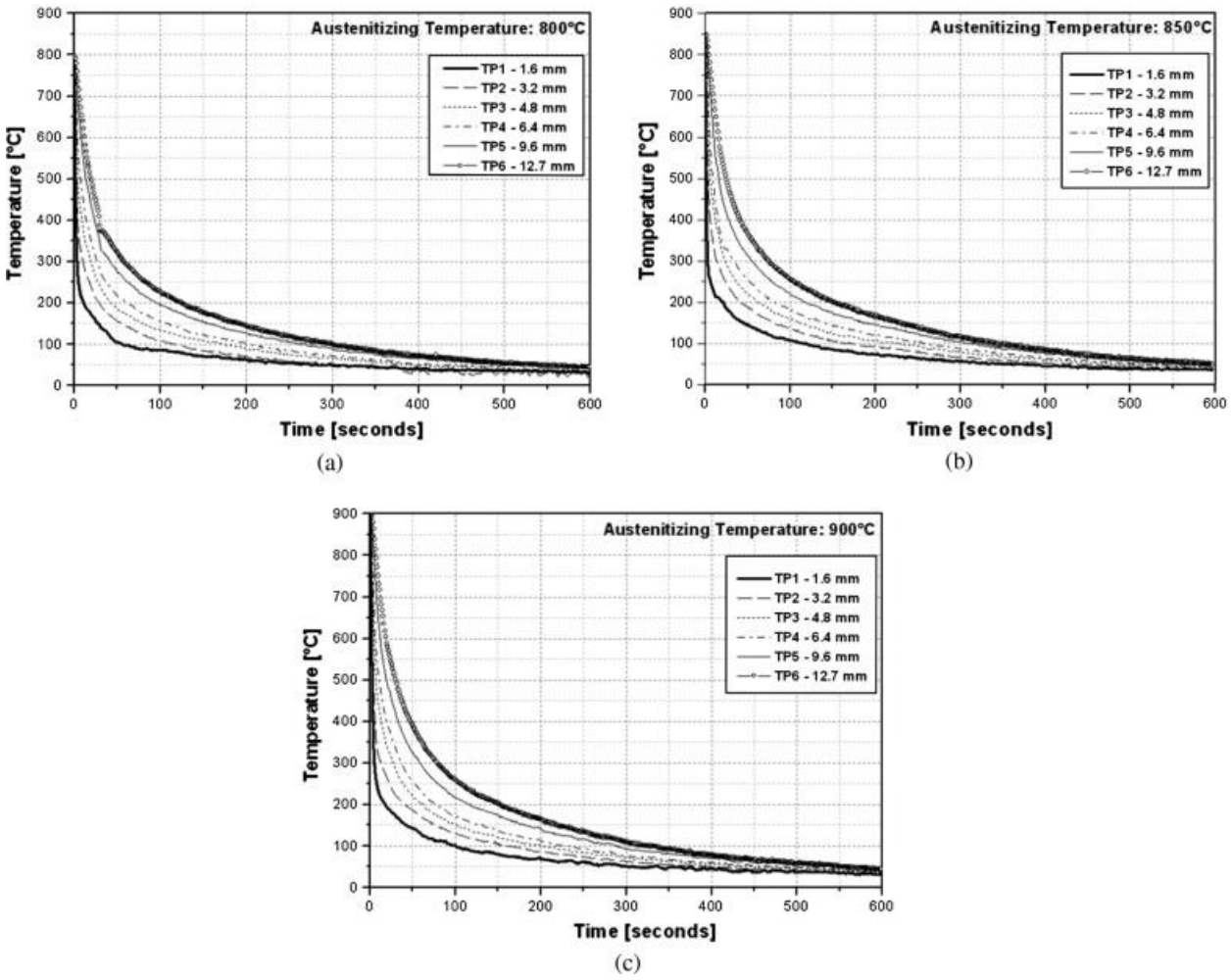

Figure 1 Cooling curves Experimental [7]

Hardness values as a function of austenitizing temperature is plotted and shown in Figure 3.

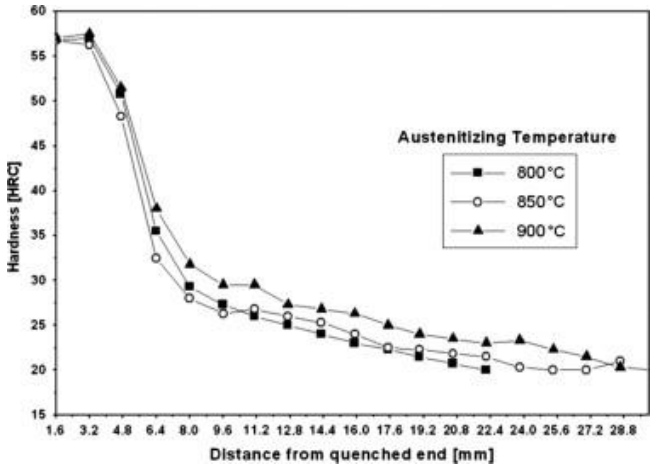

Figure 2 Hardness as a function of Jominy distancces[7]

Finally, percentage of all phases relative to Jominy distances.

Distance(mm)	Martensite	Bainite	Pearlite	∑%
1.6	100	-	-	100
3.2	87.6	12.4	-	100
4.8	71.2	14.4	14.4	100
6.4	16.4	-	83.6	100
8	-	-	100	100
12.8	-	-	100	100

Table 1 Percentage of each phase experimental [7]

Above values in Table 2 were used to compare our results with experimental data.

1.6 Hardness Calculation Models

Two mathematical models for calculation of hardness will be discussed in this thesis.

1.6.1 Ion and Anisdahl

In order to calculate the Vickers index (hardness) empirical relations as proposed by Ion and Anisdahl[6] were used. These equations are derived from experiments on different alloy steels. Following is the chemical composition limits of these steels, Carbon from 0.1 to 0.5 %, Silicon less than 1%, Manganese less than 2%, Chromium less than 3%, Molybdenum less than 1%, Nickel less than 4%, Copper less than 0.5%, Aluminum between 0.01 and 0.05%, Vanadium less than 0.2% and Mn + Ni + Cr + Mo less than 0.5%.

For Ferrite and Pearlite:

$$HV = 42 + 232C + 53Si + 30Mn + 12.6Ni + 7Cr + 19Mo + (10 - 19Si + 4Ni + 8Cr + 130V)Log(\varphi) \quad \text{............................ Equation 10}$$

For Bainite:

$$HV = -323 + 185C + 330Si + 153Mn + 65Ni + 144Cr + 191Mo + (89 + 53C - 55Si - 10Ni - 22Mn - 20Cr - 33Mo)Log(\varphi) \quad \text{........Equation 11}$$

For Martensite:

$$HV = 127 + 949C + 27Si + 11Mn + 8Ni + 16Cr + 21Log(\varphi) \quad \text{........Equation 12}$$

Unit is weight percentage of each alloying element and φ denotes cooling rate in °C/h at 700 °C. In order to find over all HV value, we need to multiply HV value for each phase with its relative fraction and then add all the values.

$$HV = \Sigma f_i \, HV_i \quad \text{......... Equation 13}$$

1.6.2 Trzaska[24] model

This model takes advantage of very popular model presented by Maynier[25] and is based on the application of following methods

- Multiple regression
- Logistic regression

The hardness affecting variables are Austenitizing temperature, mass concentration of elements and cooling rate. More than 500 CCT diagrams were processed to prepare empirical data for this model. Following are the limits on chemical composition, Carbon between 0.06 and 0.68 %, Mn 0.13 to 2.04%, Silicon 0.12 and 1.75%, Chromium less than 2.3%, Ni less than 3.85%, Mo less than 1.05%, Vanadium less than 0.38% and Copper less than 0.38%.

Binary variable W_x which shows the presence of ferrite, pearlite, bainite and martensite in the microstructure. It is calculated with following equations

$$w_x = \begin{cases} 0 & if\, S_x \leq N \\ 1 & if\, S_x > N \end{cases}$$

Equation 14

$$S_X = \frac{\exp(K_X)}{1 + \exp(K_X)}$$

Equation 15

Here X is f(ferrite), p(pearlite), b(bainite), and m(martensite). Value of N is 0.4 for bainite and 0.5 for ferrite, pearlite and martensite. Following equations are used to calculate classificators for this hardness model, Equations 14 to 19 are used to calculate the amount of phases present after cooling. In case of ferrite and pearlite, problem can be simplified by looking at highest cooling rate required for transformation. In case of martensite, lowest cooling rate for transformation is unknown. Bainite transformation has two values restricting its area of occurrence.

$K_f = 18.4 - 15.4 * C - 1.9 * Mn + 0.7 * Si - 2.5 * Cr - 1.5 * Ni - 4.8* Mo + 2.4 * V + 1.4 * Cu - 0.004 * T_A - \sqrt[4]{V_c}$ …….Equation 16

$K_p = 12 - 1.4 * C - 2.3 * Mn - 2.3 * Cr - 1.4 * Ni - 6 * Mo + 3.9*V + 1.4 * Cu - 0.002 * T - 1.2* \sqrt[4]{V_c}$ ……..Equation 17

$K_b = 1.3 - 3.7 * C + 0.45 * Mn + 0.2 * Cr + 0.18 * Ni + 1.9 * Mo - 0.17 * \sqrt[4]{V_c} - 0.57 * \sqrt{(4.35 - \sqrt[4]{V_c})^2}$ ……..Equation 18

$K_m = -16.5 + 4.7 * C + 2.6 * Mn + 0.6 * Si + 2.4 * Cr + 1.2 * Ni + 1.9Mo + 4.8 * Cu + 0.006 * T_A + 1.1 * \sqrt[4]{V_c}$ ……..Equation 19

$HV_m = 200 + 824 * C + 44 * Mn + 14 * Cr + 9 * Ni + 171 * V + 78.5 * Cu + 4.13 * \sqrt[4]{V_c}$ ……..Equation 20

$$HV_{f\text{-}p} = -73 + 253 * C + 52 * Mn + 10 * Si + 36 * Cr + 8 * Ni + 20 * Mo + 80 * V + 0.11 * T_A + 12.5 * \sqrt[4]{V_c} \quad \text{……..Equation 21}$$

Equation 20 is used for martensitic structure and Equation 21 is used for Ferrite-Pearlite structure. In addition to this Equation 22 is used to calculate hardness of steel which is cooled at particular cooling rate of V_c from austenitizing temperature T_A. There are independent variables in this model which are mass concentration of elements, austenitizing temperature, cooling rate and 4 binary variables determining the phases present in microstructure. Trzaska[24] used all three equations on different set of steels and presented results in form of graphs superimposed on experimental data.

$$HV = 3.7 + 225 * C + 82 * Mn + 28 * Si + 55 * Cr + 28 * Ni + 53.5 + mo + 147 * V + 71 * Cu + 0.09 * T_A - 3.8 * \sqrt[4]{V_c} + 68 * C * \sqrt[4]{V_c} - 42 * W_f - 69 * W_p - 32.5 * W_b + 72 * W_m \quad \text{……..Equation 22}$$

By using above equations, we can calculate hardness of steel cooled from austenitizing temperature. We will use Ion and Anisdahl model for our calculations because of its simplicity.

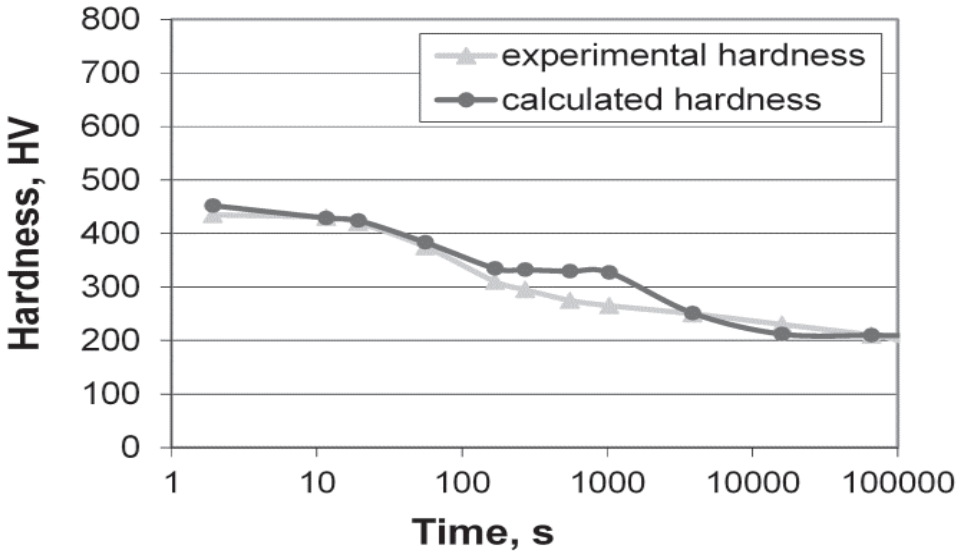

Figure 3 Hardness comparison (Experimental and Calculated values) [24]

Figure 4 shows the difference between values calculated using Trzaska model and the ones calculated using experiments for low carbon steel.

1.7 Hardness of Tempered Martensite

Grange, Hribal and Porter[26] did a systematic study of effect of carbon, manganese, phosphorus, silicon, nickel, chromium, molybdenum and vanadium on the hardness of martensite in low to medium carbon steels tempered for one hour between temperature of 204 ℃ and 704 ℃. They showed that in case of quenched steel hardness increase with increasing carbon content but when tempering effect of carbon on hardness decreases with increasing tempering temperature. The studies showed that the effect of alloying elements on tempered martensite was additive. All of the 7 elements showed increase in hardness of tempered martensite and increment depend on the percentage of alloying element present.

1.7.1 Fe-C alloys

Iron-Carbon alloys with carbon percentage from 0.12 to 0.97 were studied and hardness curves were plotted for different tempering temperatures. Since the hardness of as quenched martensite did not change significantly for a particular amount of carbon with addition of alloying elements, this means that as quenched martensite hardness is maximum achievable hardness for all alloys by quenching, meaning that the addition of alloying elements did not change retained austenite enough to affect the hardness of steel.

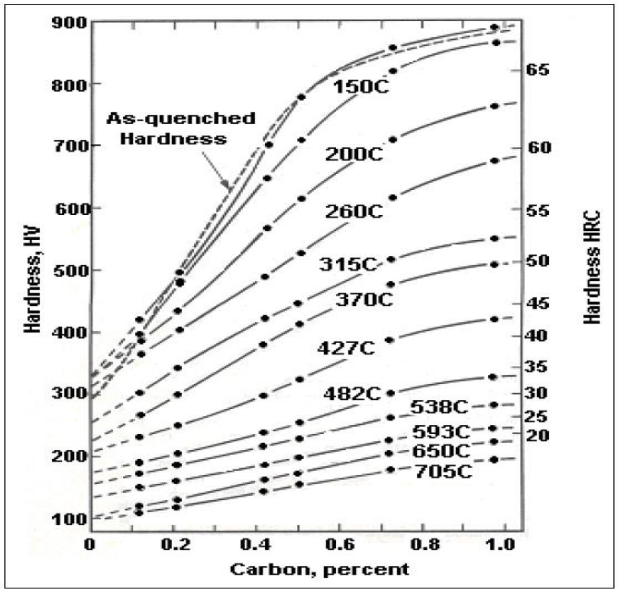

Figure 4 Hardness as a function of Carbon percentage at different Tempering temperatures [27]

It can be seen in Figure 5 that with increasing tempering temperature, carbon content does not affect hardness a lot. Figure 5 serves as a benchmark to which effect of alloying elements on hardness is studied. Below all the findings of experimental work by Hribal, Porter and Grange will be shared.

- **Fe-Mn-C**

  At 204 ℃, effect of increasing manganese on hardness of tempered martensite is negligible as compared to Fe-C alloy tempered at 204 ℃. As for tempering temperatures higher than 316 ℃, addition of manganese resulted in significant increase in hardness.

- **Effect of phosphorous**

  Similar to the effect of manganese, addition of phosphorous resulted in higher hardness at all tempering temperatures except at 204 ℃. The increase in hardness due to phosphorous was scattered about single curve at various tempering temperatures. This means phosphorous has same effect on hardness for temperature ranging between 260 ℃ to 649℃. Phosphorous does not affect carbide size, so increase in hardening is most probably due to solid solution hardening of ferrite matrix.

- **Effect of silicon**

  Silicon is found to have increased hardness at all tempering temperatures especially at 316 ℃. This is quite promising as it is due a well-known effect where epsilon carbide changes to cementite at around 316 ℃. It is also expected that increase in hardness might be due to solid solution hardening.

- **Effect of Nickel**

  Nickel has small effect on hardness of tempered martensite at all tempering temperatures. For steels containing up to 1.5 % of Nickel, the increase in hardness can be shown by a line form origin and meets 1.5% Nickel at 10 increase in HV.

- **Effect of Chromium**

  Increase in hardness due to chromium is low at 204 ℃ and keeps on increasing till 427 ℃ and then starts decreasing. Effect of chromium is more than Mn, P, Si and Nickel. The particular behaviour of chromium is due to structural changes in steel.

- **Effect of Molybdenum**

  Molybdenum is also strong carbide forming element like chromium. It also produces no effect on hardening at 204 ℃. At higher temperatures it increases hardness up to 592 ℃. Then it starts decreasing hardness due to the fact that it partitions carbide at elevated temperatures. Hence it is potent for steels at higher temperatures.

- **Effect of Vanadium**

  Vanadium has most effect of hardness increase because it is also carbide forming element. Vanadium carbides are formed when vanadium is in low quantity. At 649 ℃ hardness was maximum even though 0.18% of vanadium was added.

Figure 6 shows effect of alloying elements at different tempering temperatures. It is published in [27].

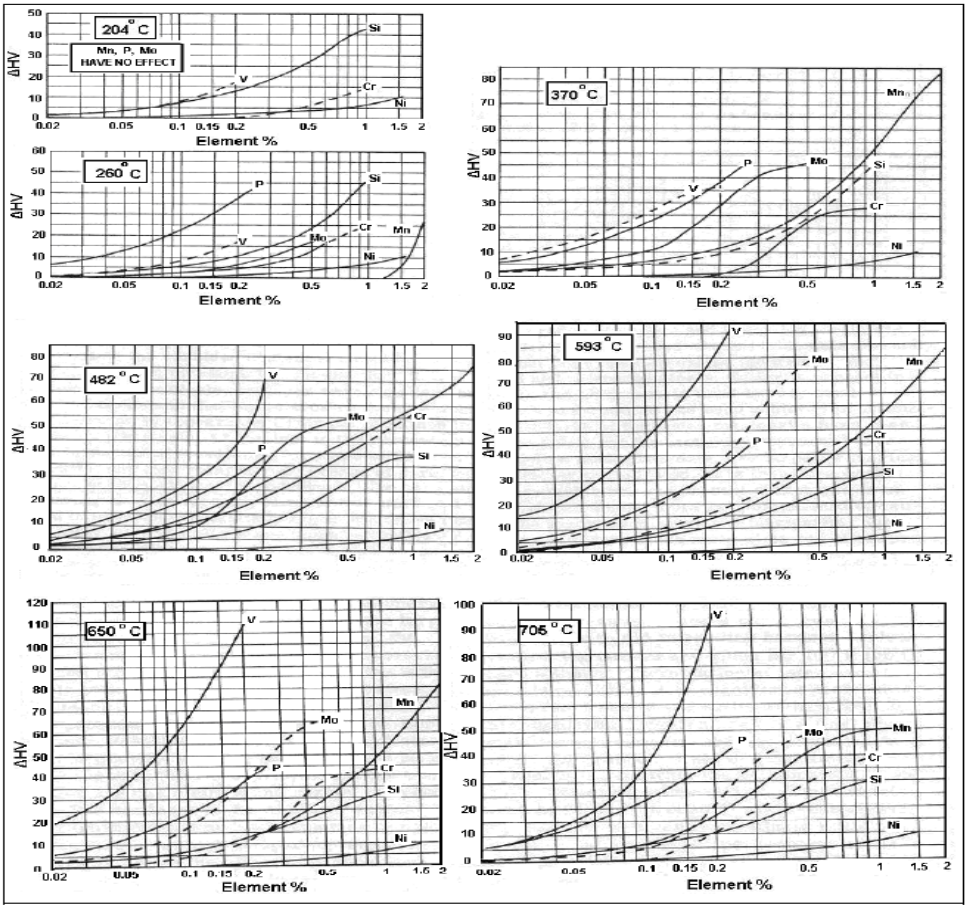

Figure 5 Effect of different alloying elements when Tempering [27]

1.7.2 Other Tempering times (Conversion)

The data presented above is for tempering time of 1 hour. It can be converted for other tempering times by using Tempering parameter. A chart is used for tempering times longer or shorter than 1 hour. The basis of this conversion is that all combinations of tempering time and temperature with same parameter will have same hardness value. Usually 1 hour tempering time is located on the chart and then by moving up or down vertically for the same parameter it is possible to read for different tempering times. For tempering time greater than1 hour we move vertically up and for tempering time lower than 1 hour we move vertically downwards. Figure 7 is published by Hribal Porter and Grange [26] in their research.

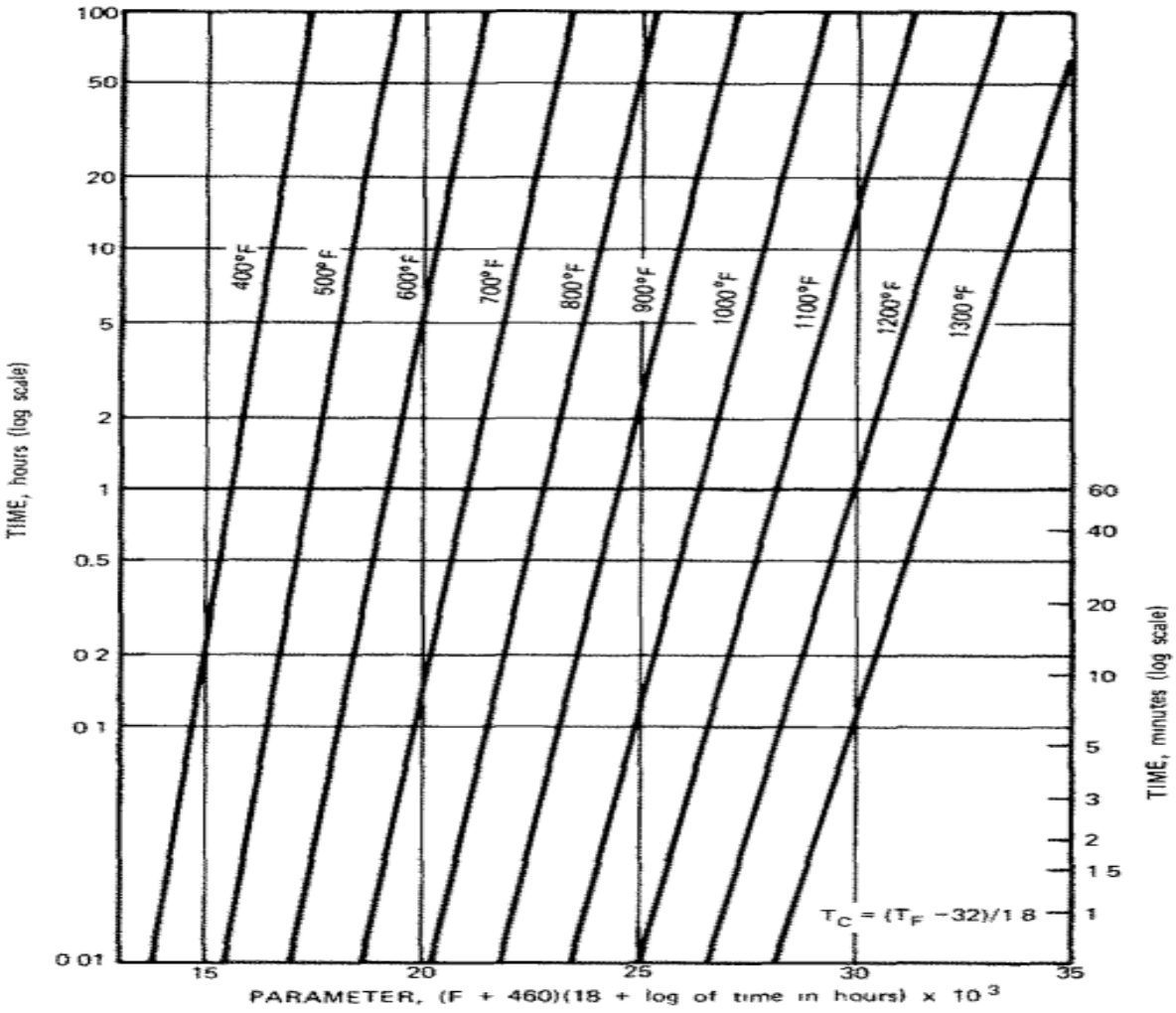

Figure 6 Tempering time conversion chart [26]

2 Jominy Test

During the simulation of Jominy test, the specimen is heated to 900 ℃ and quenched at one end using water while there is convection in air at the sides. So, heat flux will be different for both. The physics option used for software is austenite decomposition which is special case of Metal Phase transformation designed specifically for steels. While the test can be performed using metal phase transformation, the sole purpose of using austenite decomposition is to make programming a bit easier. The duration of test is kept at 2000 seconds.

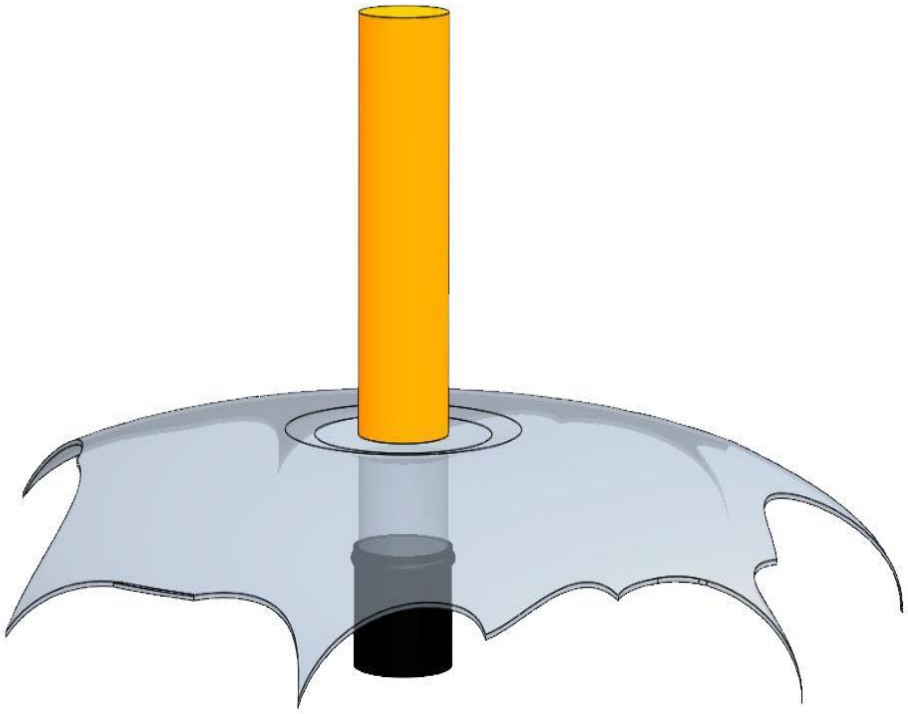

Figure 7 Jominy Test representation

At the end of simulation different phases were observed. We could see that the end which was quenched using water was almost all martensite due to rapid cooling. Austenite was almost negligible throughout the specimen.

The material used in this part of thesis, for Jominy test is C45 whose chemical composition is as follows

C	Si	Mn	P	S	Cr	Cu	Ni	V
0,44	0,22	0,66	0,022	0,029	0,15	-	-	0,02

2 Table 2 Chemical Composition of Steel

Most of data is extracted from TTT diagram of the steel which is attached below

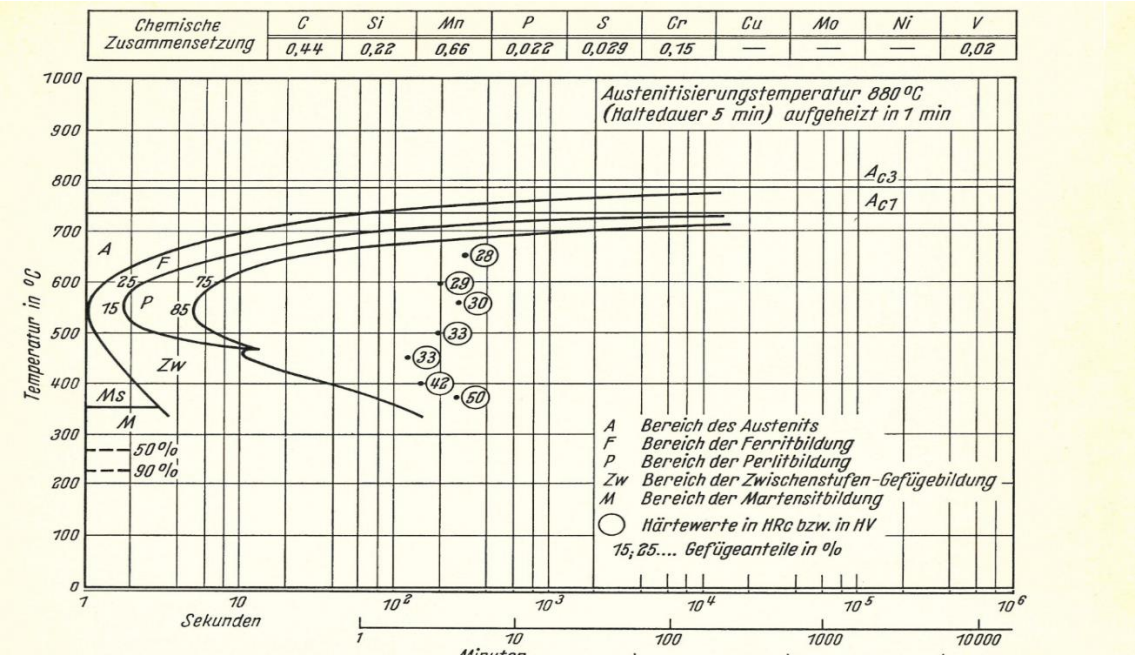

Figure 8 Time-Temperature-Transformation Diagram [1]

2.1 Models:

a) Metallurgical Model:

The metallurgical model used to simulate this problem is austenite decomposition in to other three phases which are Pearlite, Bainite and Martensite.

b) Geometrical Model:

The geometrical model used is polygon rotated along an axis, this gives us 3D shape with head dimension equal to 30 mm, core body 25 mm and main length is 100 mm. This allows much efficient and faster simulation.

c) Thermal Model:

- **Axial symmetry**

In order to obtain results in cylindrical form, axial symmetry is implemented with thermal insulation on symmetry axis.

- **Thermal Properties**
  Density is kept at constant value of 7800 kg/m^3
  Thermal conductivity (K) and **Heat capacity (c_p)** is a function of temperature and phase. Values are linearly interpolated using data provided in literature. Results are provided in Tables 3, 4 and 5.

Temperature (deg C)	K [W/(mK)]	C_p [J /(Kg.K)]
0	52.33	418.60
100	51.28	484.01
200	50.23	549.41
300	46.05	585.09
400	41.86	620.76
500	38.20	687.70
600	34.53	762.45
700	30.87	837.20
800	27.21	1004.64
900	20.93	1444.17
1000	14.65	1883.70

Table 3 K and Cp values of Bainite, Pearlite and Martensite [2]

Temperature (deg C)	K [W/(mK)]	C_p [J /(Kg.K)]
0	14.65	502.32
100	15.91	527.44
200	17.16	552.55
300	18.42	577.67
400	19.67	602.68
500	20.93	627.9
600	22.19	632.09
700	23.44	636.27
800	24.70	640.46
900	25.95	644.46
1000	27.20	648.83

Table 4 K and Cp for Austenite [2]

Variable	Austenite to Pearlite	Austenite to bainite	Austenite to martensite
$\Delta H_{s\to d}$	587714400 J/m^3	587714400 J/m^3	653016000 J/m^3

Table 5 Latent heat of phase Transformation [2]

- **Thermal cycle**
  Completely austenitic steel specimen at 900 degC is cooled from one end with water with heat transfer coefficient value of 18000 W/(m^{2}K) [3] and air on other sides with heat transfer coefficient value of 39 W/(m^{2}K) [3]. Both fluids are at 20 degC.

2.2 Phase Transformation model

- **Austenite to Pearlite and Bainite:**

  Johnson-Mehl-Avrami-Kolmogorov(JMAK) model was used to calculate fraction of phase transformation. It is based on avrami equation

$$\xi^d = \xi^d_{eq}\left(1 - exp\left(-\left(\frac{t}{\tau_{s\to d}}\right)^{n_{s\to d}}\right)\right)$$

Equation 23

τ and n are functions of temperature. ξ^d is the destination phase.

Software use differential form of equation which is as follows

$$\dot{\xi^d} = \left(\xi_{eq}^d - \xi^d\right)\frac{n_{s\to d}}{\tau_{s\to d}}\left(-\ln\left(1-\frac{\xi^d}{\xi_{eq}^d}\right)\right)^{1-1/n_{s\to d}}$$

Equation 24

This formula defines as a function of temperature, the transformation speed and the phase fraction already transformed.

After working on the Avrami law we can simplify it by setting equilibrium phase equal to 1 and consider z to be destination phase. It is possible to solve this equation for 1% and 99% curves to get two equations and two unknowns. Solving for different values of temperature we can get values of n and τ.

$$z = 1 - exp\left(-\left(\frac{t}{\tau}\right)^n\right)$$

Equation 25

Solving for 1% and 99% points on curves

$$\begin{cases} \left(\frac{t_1}{\tau}\right)^n = -\ln(1-0.01) \\ \left(\frac{t_2}{\tau}\right)^n = -\ln(1-0.99) \end{cases}$$

Equation 26

Further simplifying these equations by each other to isolate n

$$n\ln\left(\frac{t_1}{t_2}\right) = \ln\left[\frac{\ln(0.99)}{\ln(0.01)}\right]$$

Equation 27

By finding two variables for different values of temperature we can use JMAK model in software to simulate our problem. The above method is used for both Bainite and Pearlite modelling.

The values are given in Table 6 and Table 7.

Temperature[degC]	n	τ
710	1.04	2334
700	1.33	317.75
675	1.22	260.4
650	1.56	76.33
625	1.6	35.45
600	4.4	5.67
550	3.8	3.35
500	4.07	4.80
470	3.11	6.144

Table 6 n and tau for pearlite

During simulation temperature limits were set in order to get more accurate results. In case of pearlite, it is set to be between 550 and 710 deg C. This prevents software from interpolation beyond these limits. To prevent error discussed in previous section (1.4.2), initial phase value of 0.01 is selected for both Bainite and Pearlite.

Temperature[degC]	n	τ
470	3.11	6.14
400	1.9	22.51
375	1.83	30.87

Table 7 n and tau for bainite

In case of Bainite the temperature limits are set to be between 375 and 470 degree centigrade.

- **Austenite to Martensite**

Different kind of model is used known as Koistinen Marburger model. Its equation is as follows

$$\xi^d = \xi_0^s \left(1 - exp\left(-\beta(M_s - T)\right)\right)$$

Equation 28

β is Koistinen Marburger coefficient.

M_s is the start temperature for martensite.

$$z=1-e^{(-\beta(M\_s-T))} \quad \text{……. Equation 29}$$

in case of 99% curve, we get

$$\beta = -\ln(0.01)/(M_s - T) \quad \text{…….Equation 30}$$

In our case β is 0.014[1/K] because M_s is 350 degC. ΔMs[K] is start temperature smoothing, which is equal to 5, it makes onset of transformation smooth.

In this case also software uses a differential formula which is derived from

$$\dot{\xi}^d = -\xi^s \beta \dot{T}$$

Equation 31

2.3 Results (Jominy Test):

The temperature on different points at different depths of specimen are plotted against log of time. It can be seen in the plot that at the base of specimen towards the end where water quenching is done, the temperature drops much quickly hence resulting in the formation of martensite. On the contrary, as we move towards the other end temperature drop is much slower for example in case of 80 mm, we can see the drop in temperature is less sudden The graph is presented in Figure 9.

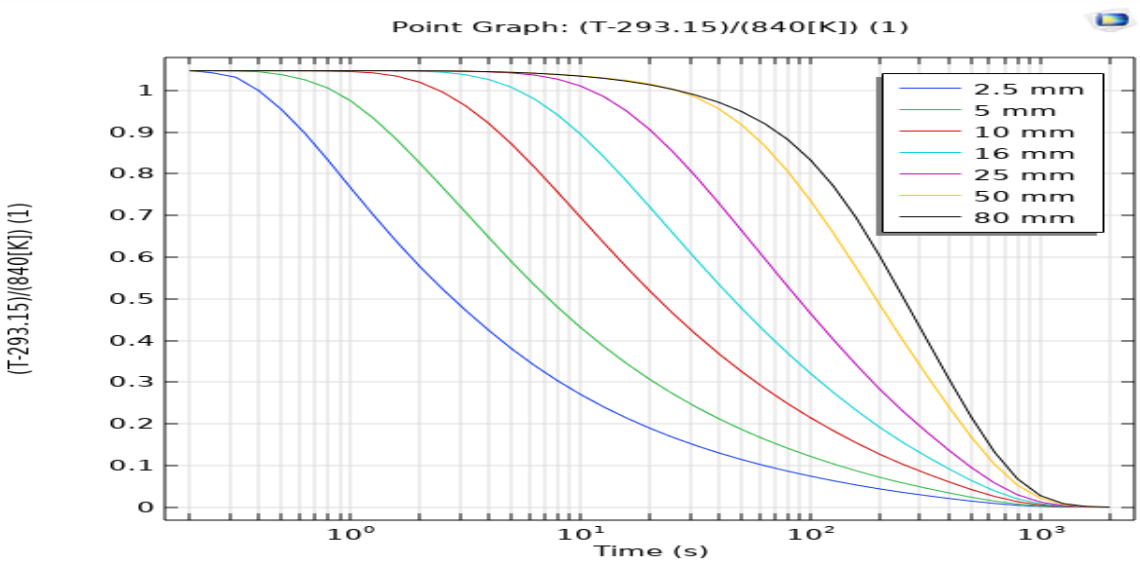

Figure 9 Temperature profile at different Jominy distances

This graph is very similar to that of provided in Iso standard.

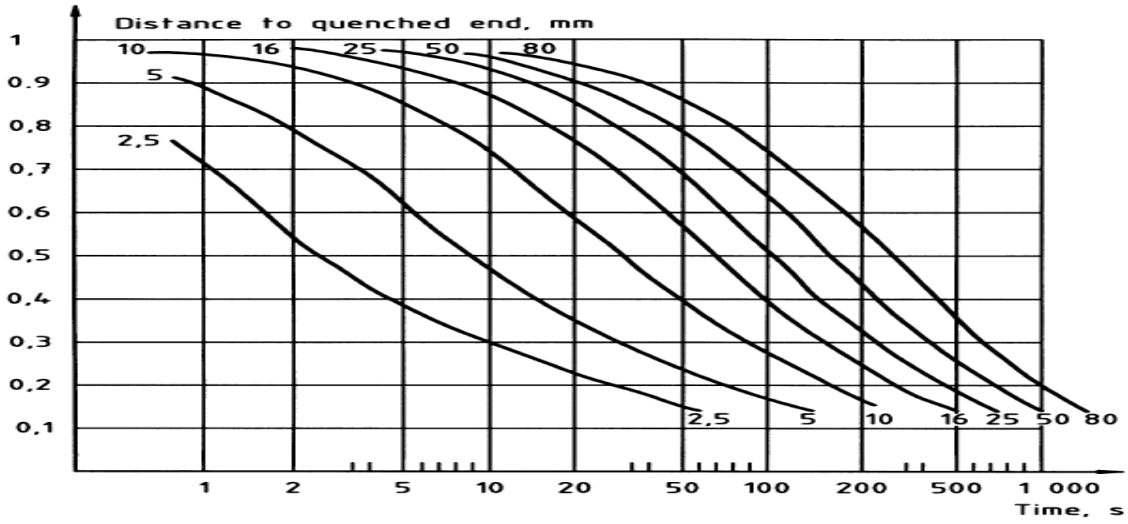

Figure 10 Temperature profile Experimental [8]

Figure 10 is taken from British standard of Jominy test (BS EN ISO 642:1999). It is evident from both Figure 9 and Figure 10 that the results are almost same.

Another plot is presented in Figure 11 which shows cooling rate at different Jominy distances. The points taken are same as those presented in Figure 12. Figure 11 is better in understanding that the cooling rate depends on Jominy distances, faster towards the water quenching end and slower as we move away from it. A plot taken from [7] is presented in Figure 12 for comparison. Both graphs are almost identical.

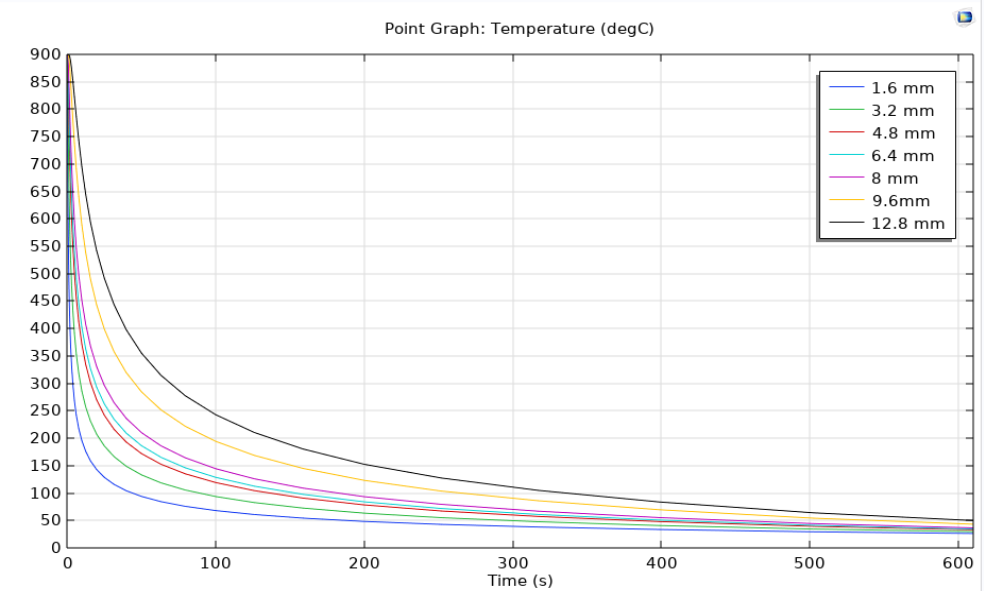

Figure 11 Cooling curves at different Jominy distances

This graph is compared with the one from litera

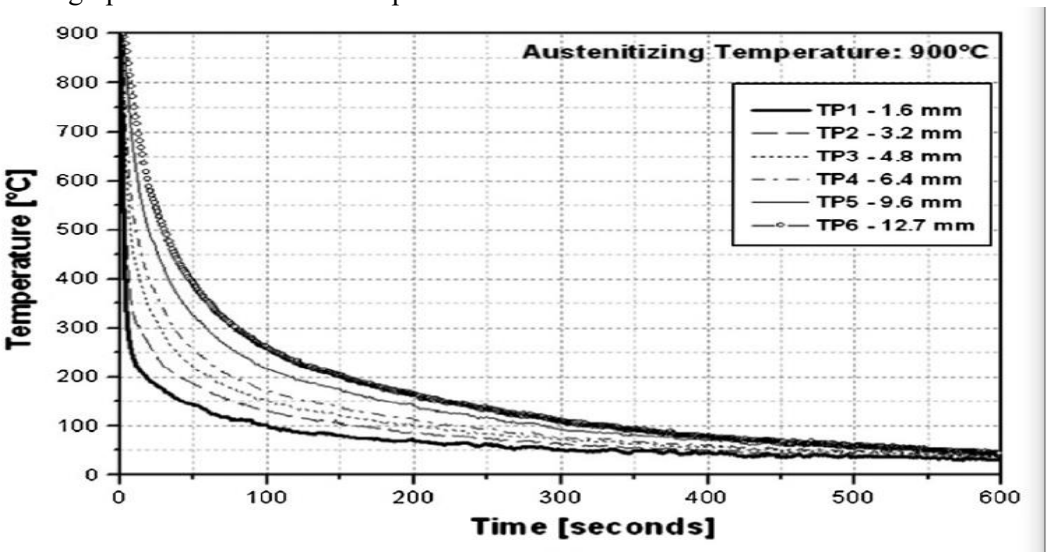

Figure 12 Cooling curves Experimental [7]

2.3.1 At 10 seconds:

Figure 13 shows the phase fraction of each phase 10 seconds into the test. We can observe that the end which is water quenched is almost completely martensite. Above martensite is a bit of pearlite. Almost everywhere else austenite is still dominant.

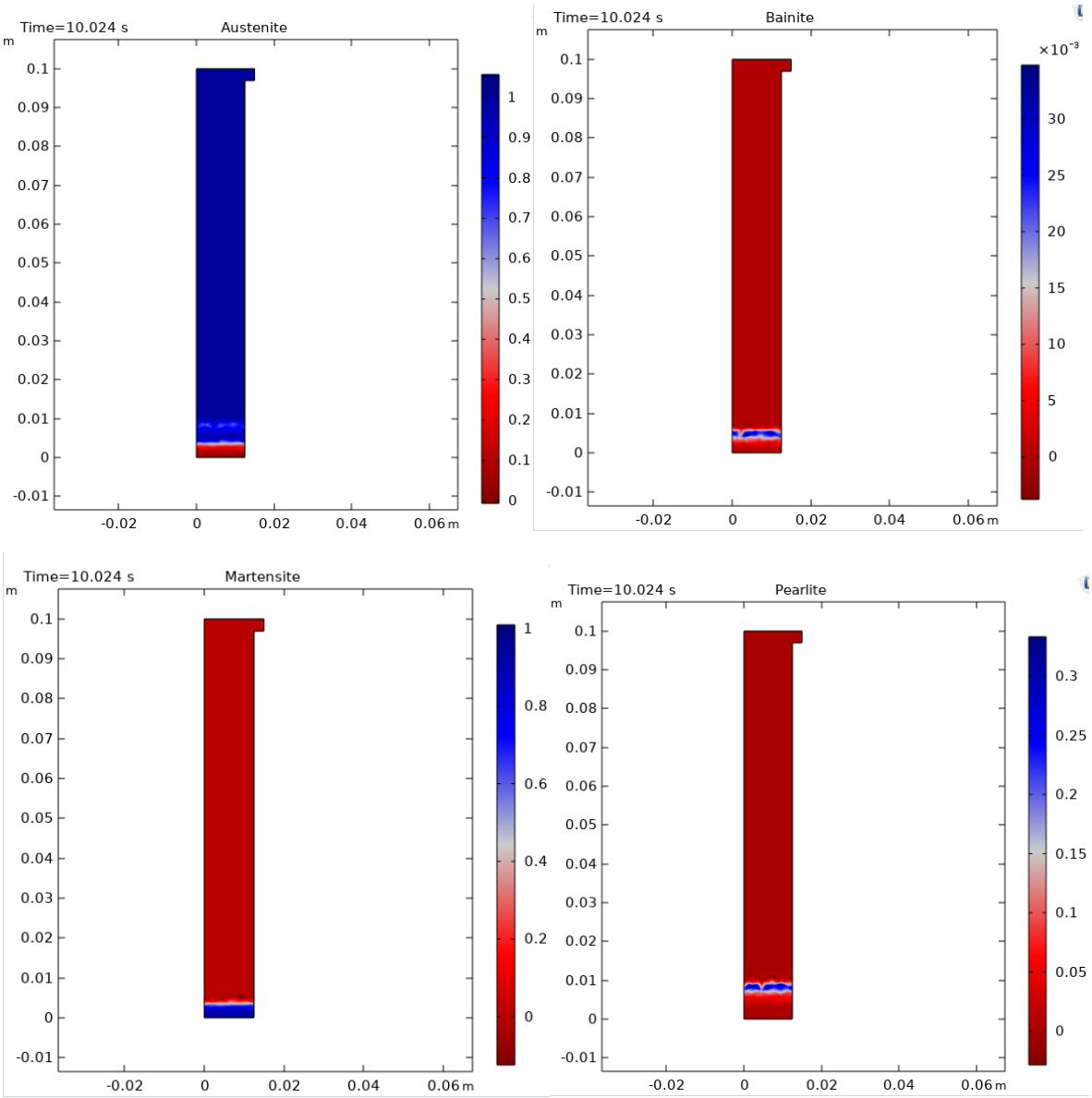

Figure 13 Percentage of all phases at 10 seconds in to the test

2.3.2 At 2000 seconds:

The percentage of phase fraction at the end of test is shown in below in Figure 14. As expected, Martensite is the dominant phase at the end which is being quenched by water. This is due to extremely fast cooling. Above that is a bit of Bainite and everywhere else its pearlite.

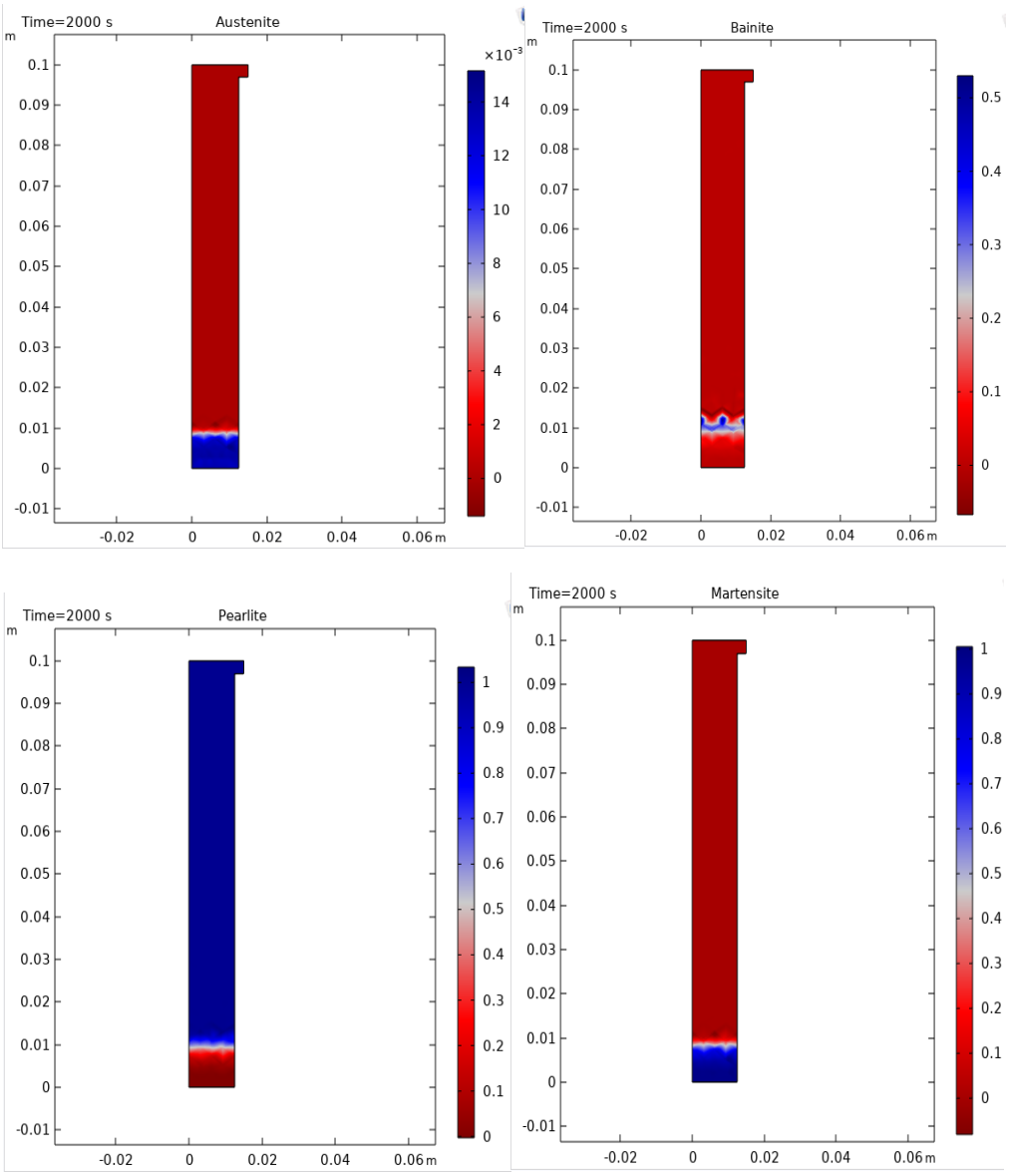

Figure 14 Percentage of all phases at 2000 seconds

2.3.3 Hardness Calculation:

The first step in calculation of hardness is getting cooling rate at 700°C on different depths of specimen. Then from these values and by using the equations proposed by Ion and Anisdahl, Vickers index for different phases at different distances is calculated. Finally, each value of Vickers index is multiplied by relative fraction and all of the results are added to get total value of HV. These results are stated below in form of Table 8. These HRC values are rounded off.

Distance(mm)	f_b . $HV_{bainite}$	f_p . $HV_{pearlite}$	f_m . $HV_{martensite}$	HV	HRC
1.6	0	0	631.2	631	57
3.2	7	0	612	631	56
4.8	11.67	6.27	574.4	592	55
6.4	21.02	20.92	505	547	52
8	46.76	41.83	378.8	467	47
9.6	60.8	104.6	151.5	317	32
12.8	0	205	12.63	218	15

Table 8 Hardness calculation at different jominy distances

To get better understanding and to compare results with literature, a graph is plotted between distance and HRC values presented in Figure 15.

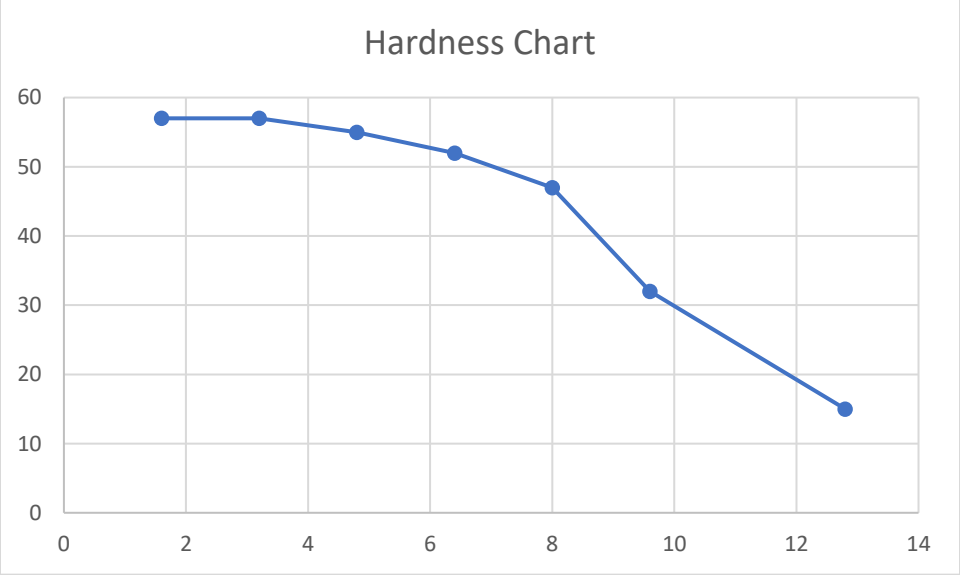

Figure 15 Hardness as Function of Jominy Distances

Figure 16 shows experimental hardness values and it is taken from literature [7]

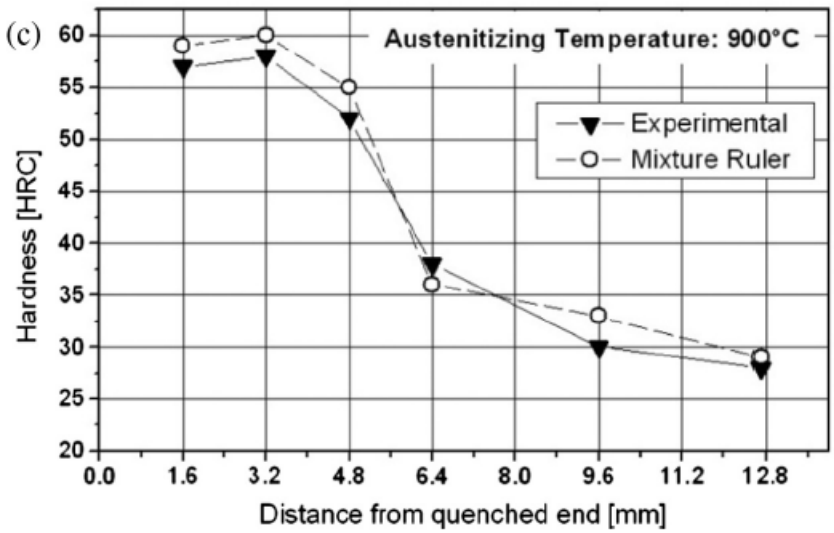

Figure 16 Hardness against Jominy Distances Experimental [7]

2.2.3.2 Hardness Calculation using standard[8]:

The ASTM A255 internattional standard identifies value of hardness at different Jominy distances. This method of calculating value of hardness using Ideal diameter was originally used by M A Grossman and further improved by refinement of carbon multiplying factors and correlation of Boron factors. By using the table provided in standard value of DI was calculated to be 1.12 inches(28.5mm). Initial hardness of 0.44% carbon alloy at 100% martensite is 58 HRC. By applying interpolation on given table value of factors and hence relative hardness at different Jominy distances was calculated. Table 9 shows hardness at different points calculated by using standard.

Jominy Distance(mm)	Factor	HRC
0	1	58
3	1.1	52
5	1.51	38
7	1.95	30
9	2.45	24
11	2.65	22
13	2.79	21

Table 9 Hardness calculation by standard

The results are presented in graphical form in Figure 17 for better understanding and easy comparison

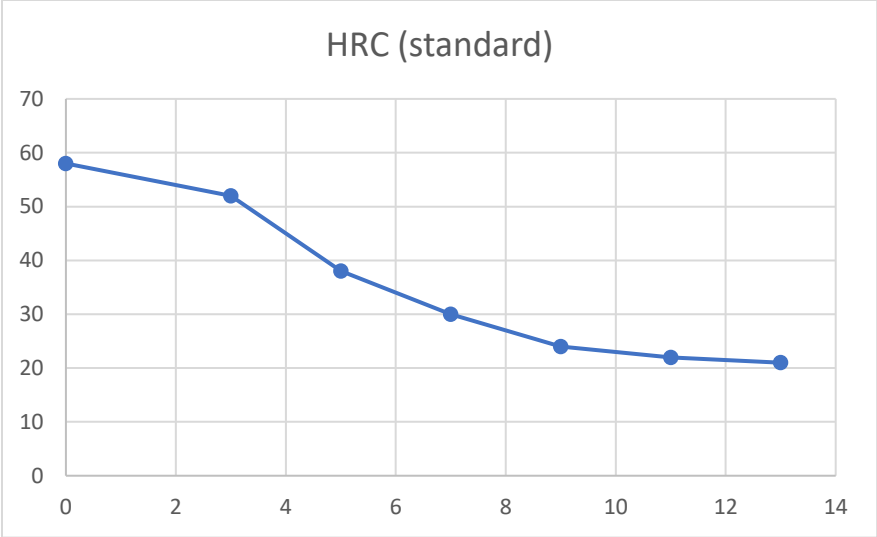

Figure 17Hardness against Jominy distances calculated using standard [8]

2.2.3.3 Hardness Comparison

Finally, an overlap of all three types of values which are obtained from simulation, Experiment and Standard is plotted below in Figure 18.

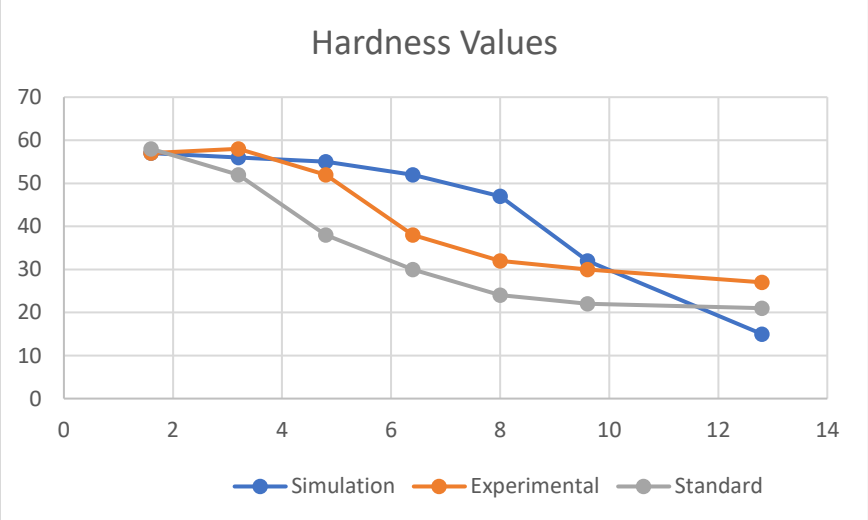

Figure 18 Simulated(Figure 15) , Experimental[7] and Standard [8] superimposed on eachother

The values obtained using simulation are a bit higher than the ones obtained through experimental and Standard. This could be the result of inaccurate or non-updated data of CCT diagram. Nevertheless, the results are quite promising at beginning and end of simulation.

3 Time quenching (Quenching and Self tempering)

Time quenching is a process where long infinite bar heated at around 950 [deg C] is quenched in water until surface temperature fall below certain value and then the bar is cut into desired length and left to cool by air convection. This is beneficial because surface of bar becomes martensite and then due to high temperature in core temperature of surface also increases. This cause self-tempering of martensite.

This process is also referred to as The TEMPCORE process. It has three stages, in the first stage specimen is quenched using water and the cooling temperature at a certain depth is less than the critical temperature of martensite formation. This allows bar to have austenite core surrounded by Martensite layer. The thickness of martensite layer is function of quenching time.

In the second stage specimen leave quenching area and left in air for slow cooling. This causes the core which is at higher temperature to reheat surface martensite layer due to conduction, as a result self-tempering of martensite occurs. The name of process is derived from this phenomenon.

In the final stage the bar is left on cooling bed. The remaining austenite is transformed into ferrite and pearlite or ferrite, pearlite and bainite depending upon chemical composition of steel, specimen diameter, duration of quenching and efficiency of the whole process.

All of these stages are depicted in figure 19.

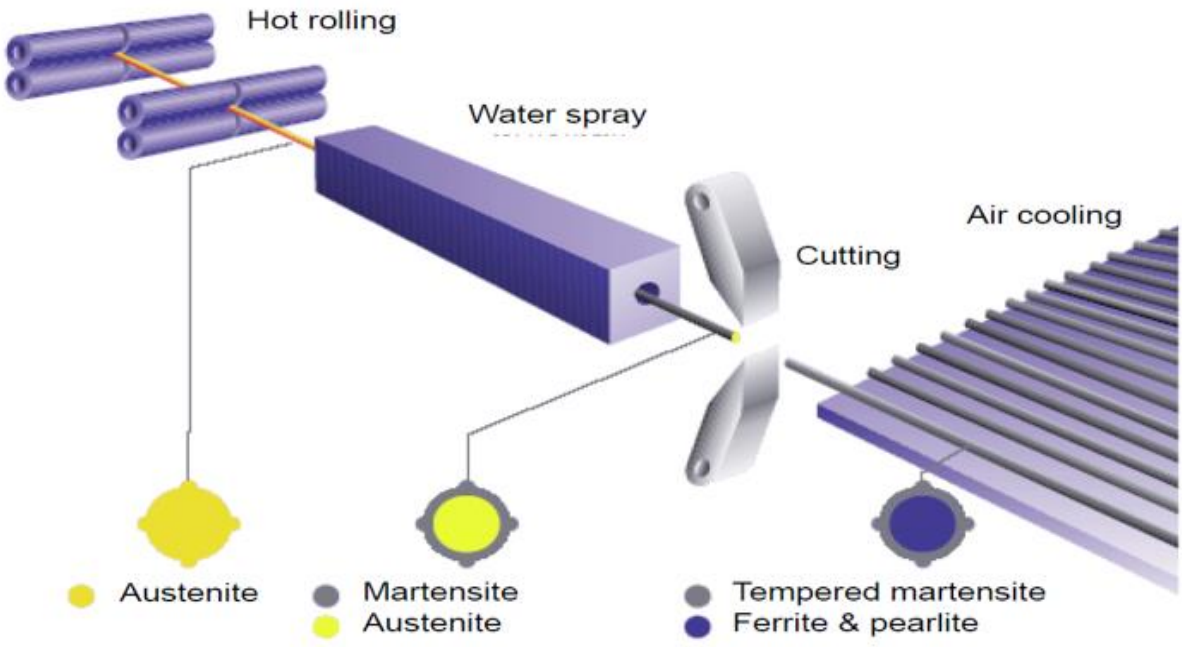

Figure 19 TempCore or Time quenching process

3.1 Models:

a) Metallurgical Model:

Same metallurgical model is used as in Jominy test. Austenite decomposition into other three phases which are pearlite, bainite and martensite.

b) Geometrical Model:

The geometrical model used in this case is an axisymmetric with height 32 mm and width 16mm. This allows for very efficient and faster simulation.

c) Thermal Model:

- **Axial symmetry**
  In order to obtain results in cylindrical form, axial symmetry is implemented with thermal insulation on symmetry axis. Also, the top and bottom surface is insulated. This is to optimize our simulation. As already mentioned infinitely long hot rolled bar is fed to quenching area, after quenching its cut to small pieces of required dimensions. This means that only heat flow rate on circular faces of cylinder is due to conduction but there is not much difference in temperature on corresponding points of 2 cylinders. This means negligible heat flow rate. Insulation allows us to take care of this effect and simplify simulation a lot.

- **Thermal Properties**
  Density is kept same as in previous simulation; its value is 7800 kg/m^3
  Thermal conductivity (K) and **Heat capacity (c_p)** is a function of temperature and phase. Values are linearly interpolated using data provided in literature. These values will remain same as that of previous problem.

- **Thermal cycle**
  At 950 deg C completely austenite steel is quenched in water under controlled cooling rate for 1.3 seconds and then left air for cooling. In the 2nd simulation water quenching duration is 1 second. Heat transfer coefficient of water and air is 18000 $W/(m^2K)$ [3] and 39 $W/(m^2K)$ [3] respectively. Both are at room temperature.

3.2 Material:

The material used is 1020 steel and it consists of various major elements along with Fe, which are C, Mn, P, S and Si. Its composition is as follows.

	C	Si	MN	P	S
1020	0.17	0.22	0.79	0.036	0.041

3.3 Kinematics of phase transformation:

Similar to our previous simulation JMAK model was implemented in FE simulation here as well. The JMAK model in isothermal conditions is expressed as follows

$$f = 1 - \exp(-bt^n)$$

Equation 32

Here f is transformed phase fraction, n is Avrami exponent, k is kinetic coefficient and t is time of transformation.

Values of n and tau are calculated using the formulas given by Cetinal et al.[5], the reason to use this data is because the results for this data are published by Cetinal [5] which gives us a base to compare our results.

$$\log b = c_{b0} + c_{b1}T + c_{b2}T^2,$$
$$n = c_{n0} + c_{n1}T + c_{n2}T^2,$$

Equation 33

The values of constants in our case are known

1. **For Pearlite**

$$\log b_{\mathrm{p}} = -22.02 + 0.06455T - 0.5142 \times 10^{-4}T^2,$$

Equation 34

$$n_{\mathrm{p}} = -34.48 + 0.1184T - 0.949 \times 10^{-4}T^2.$$

Equation 35

2. **For bainite**

$$\log b_{\mathrm{b}} = -44.05 + 0.1697T - 0.1686 \times 10^{-3}T^2,$$

Equation 36

$$n_{\mathrm{b}} = 17.28 - 0.06547T + 0.6957 \times 10^{-4}T^2.$$

Equation 37

Here b is

$$K = b = \left(1/\tau\right)^{n}$$

Equation 38

Using above equations values of n and tau are calculated for pearlite and bainite, Table 10 and Table 11 respectively.

1. **Pearlite**

Temperature	n	τ
500	0.995	410
550	1.93	11.84
600	2.39	5.67
650	2.38	5.63
700	1.89	11.87
750	0.938	499.52

Table 10 n and tau for pearlite 1020 steel

2. **Bainite**

Temperature	n	τ
500	1.93	7.6
550	2.31	5.53
600	3.04	9.17
650	4.11	16.26
700	5.54	26.38
750	7.31	38.77

Table 11 n and tau for Bainite 1020 steel

Since martensite phase transformation does not depend on time but on temperature because in this case there is no diffusion. So, the volume fraction is calculated by parabolic equation presented in [5].

$$W_m = W^*\left\{1 - \left[\left(T - M_f\right)/\left(M_s - M_f\right)\right]^2\right\}$$
$$W^* = 1 - \left(W_{F/P} + W_B\right),$$

Equation…..39

Here W_b is bainite ratio and $W_{F/P}$ is Ferrite + Pearlite ratio. W_m is martensite ratio.

For each node cooling curves were plotted by using software.

For martensite phase transformation Koistinen-Marburger equation was used in our case. This is done because data is given in [5] is in the form of curves plotted using computer program and it is much easier to apply Koistinen-Marburger equations.

B is calculated using Equation 30, for which data is extracted from the TTT diagram present in [5]. M_f is 200 ℃ and M_s is 450 ℃, the value of β in this case was calculated to be 0.018.

3.4 Results:

Results for both Tempcore process simulations 1.3 second quenching time and 1 second quenching time are presented below.

3.4.1 Quenched for 1.35 seconds

At the end of water quenching, surface of specimen is completely covered in martensite due to rapid cooling. Austenite is still present everywhere else because it is very early into experiment. Figure 20 shows the all the phases present at end of quenching.

At 1.3 seconds percentage of all phases

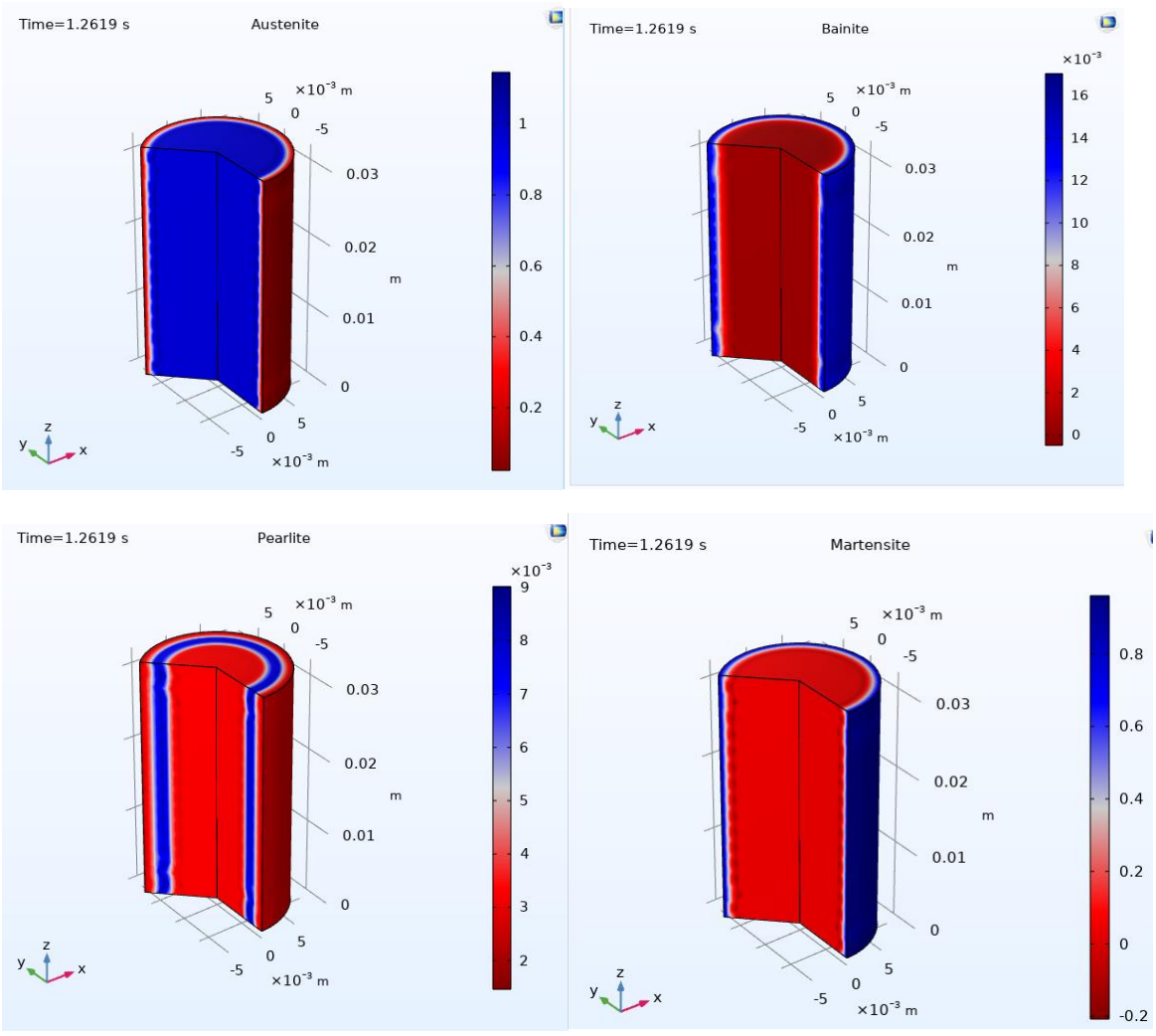

Figure 20 percentage of all phases after 1.3 seconds quenching

At the end of simulation:

At the end of simulation all of austenite is transformed in to other three phase. Surface is covered in martensite while on the inside bainite and pearlite are present in excess. Results are presented in Figure 21.

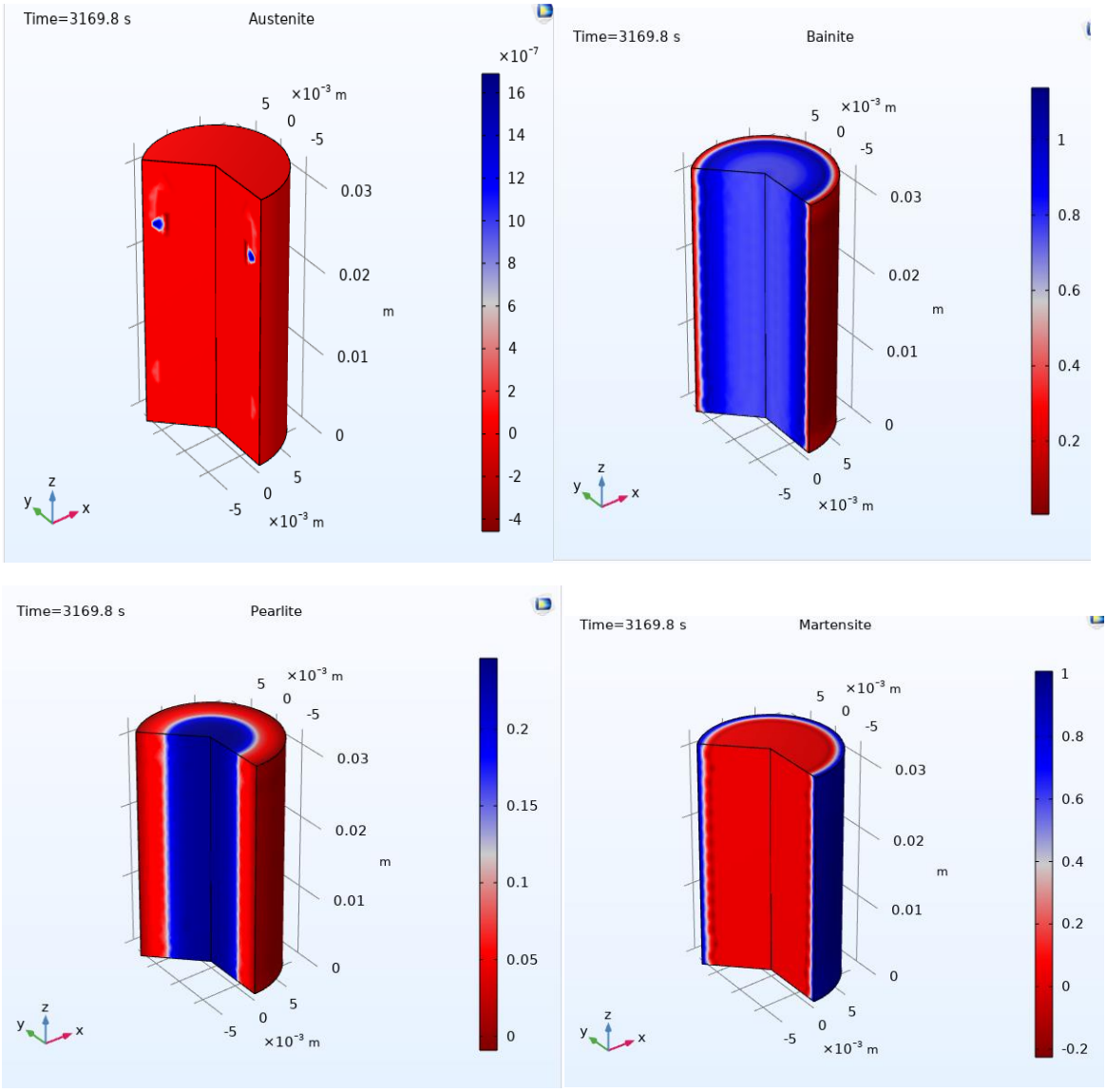

Figure 21 Percentage of all phases at the end of simulation for 1.3 seconds quenching experiment

Phase fraction against radial distance:

Phase fraction as a function of radial distance is plotted for all 4 phases in Figure 22

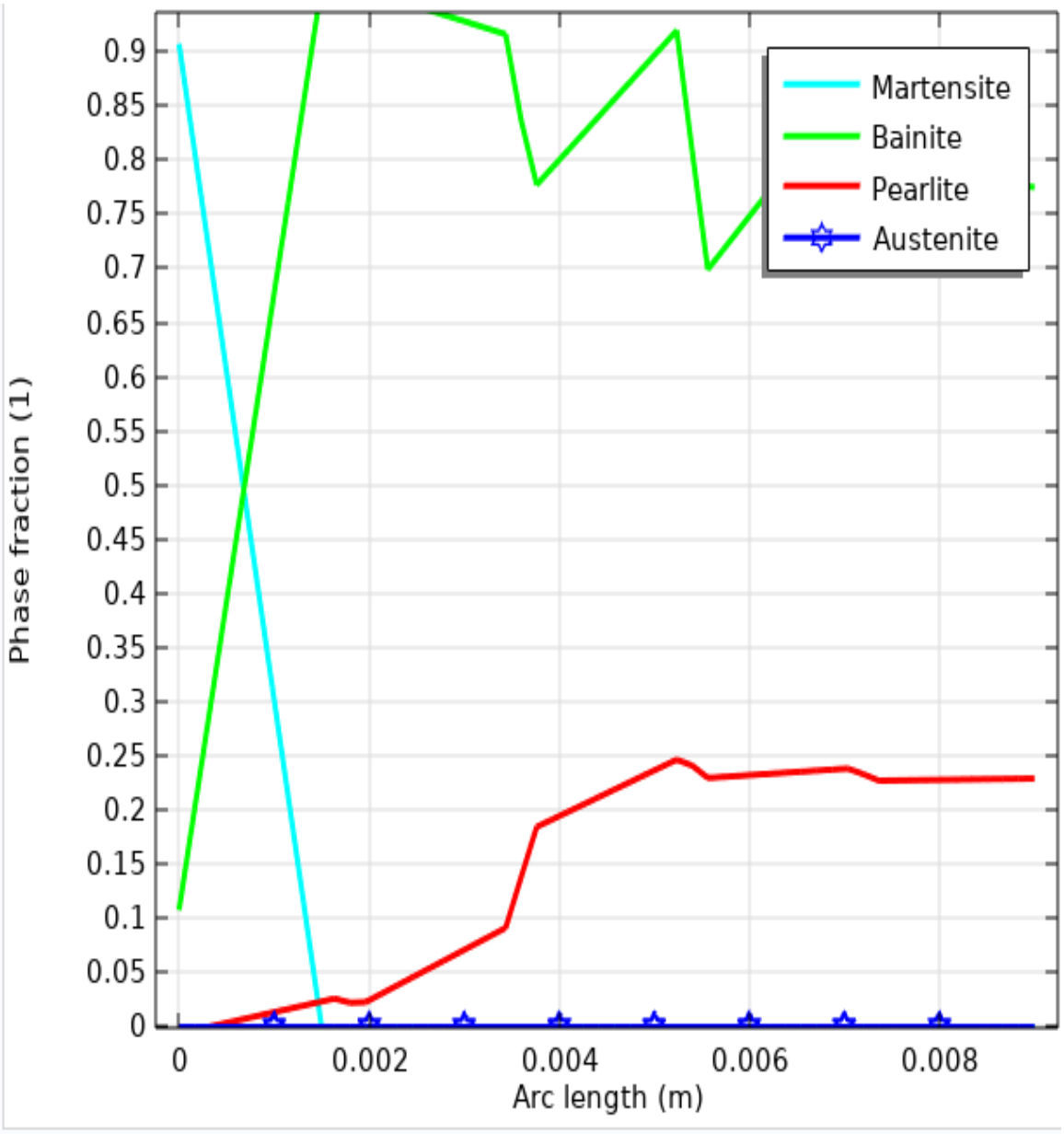

Figure 22 Phase fraction as a function of radial distance

Phase fraction against time:

Phase fraction for each phase at surface is plotted against time and presented in Figure 23.

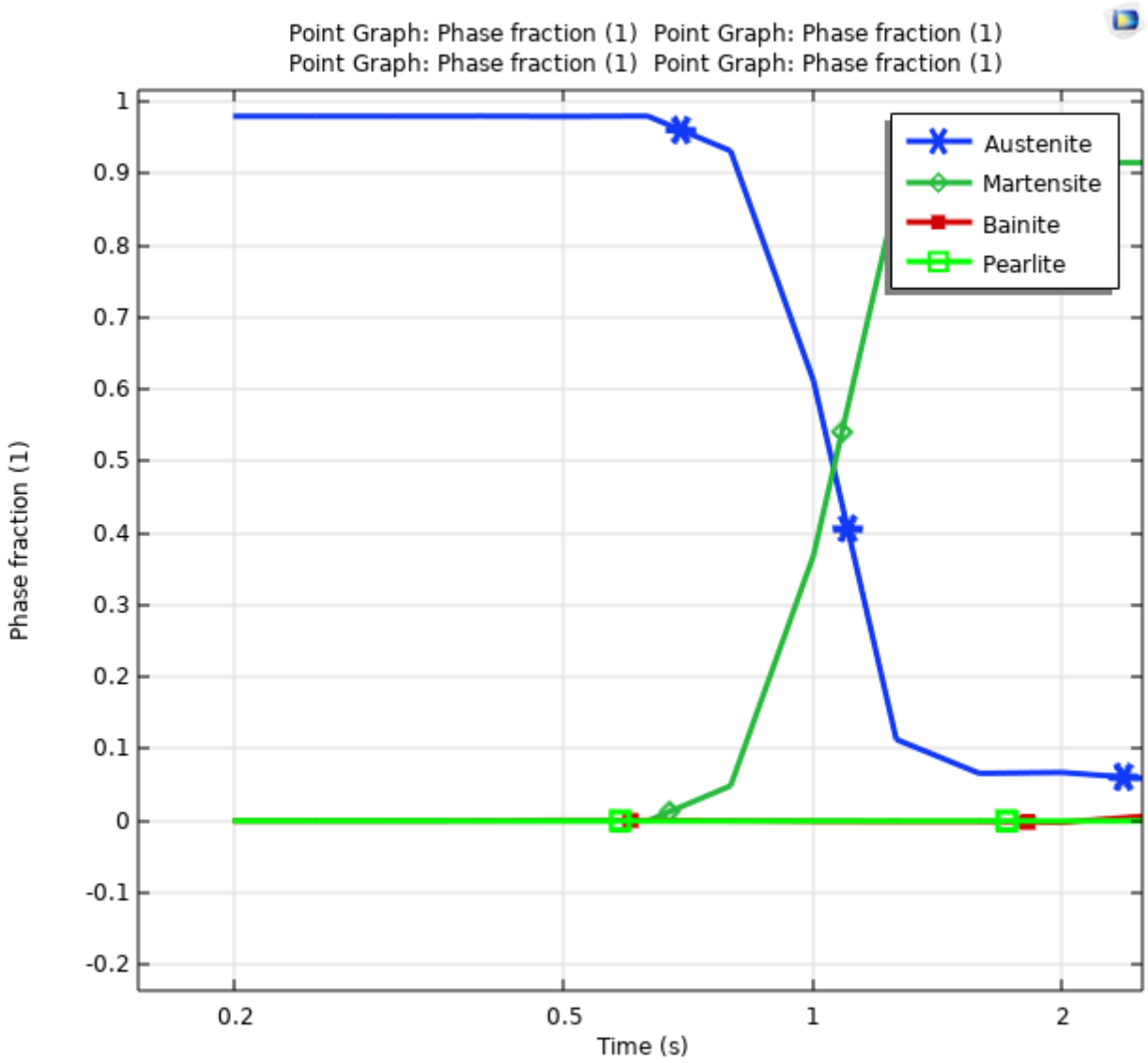

Figure 23 Phase Fraction at surface

Temperature against time curve:

This plot in Figure 24 and Figure 25 shows the temperature at different time in core and surface. We can see that the surface temperature drops below martensite threshold and then increases due to heated core hence activation the temp core process also known as self-tempering.

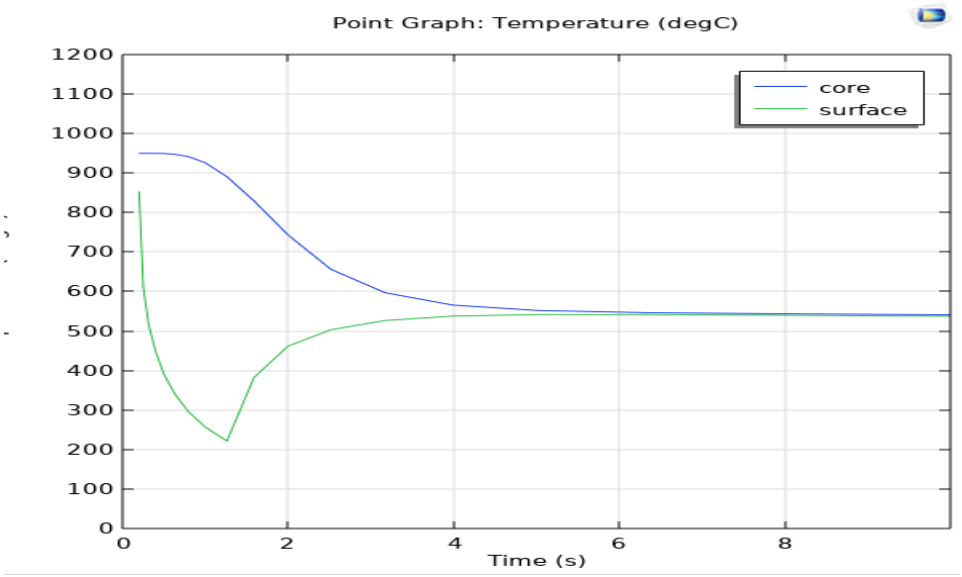

Figure 24 Temperature at Surface and core plotted against time

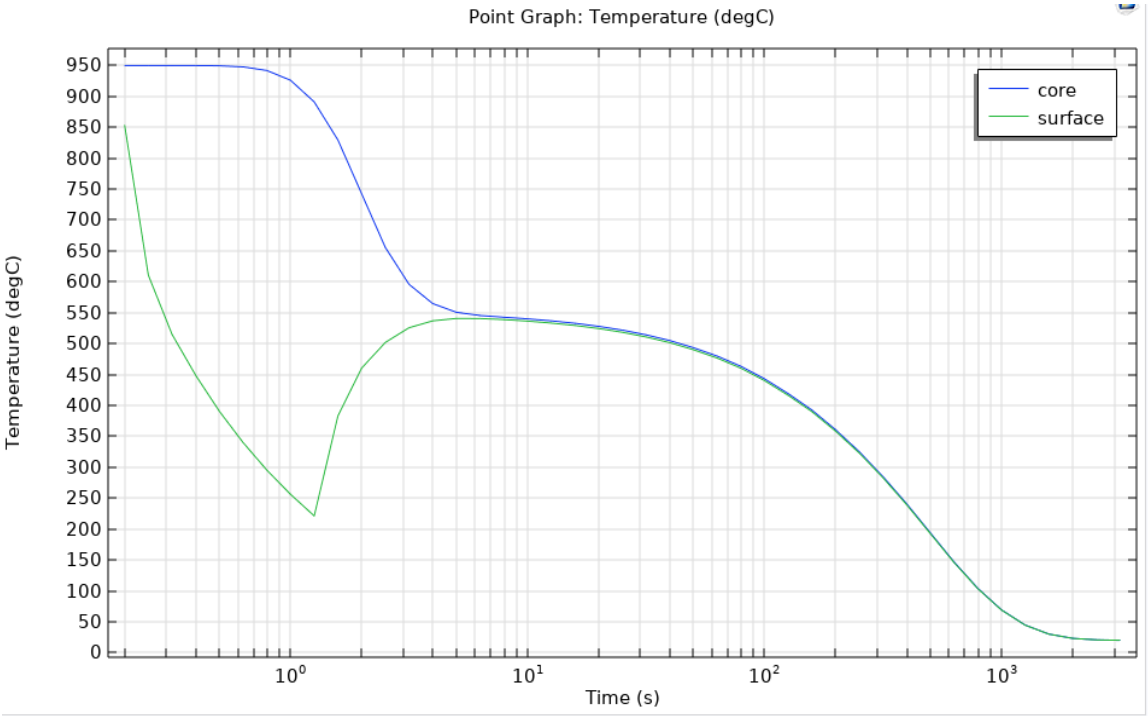

Figure 25 Temperature at Surface and Core plotted against time log scale

Figure 25 shows that the time it takes for specimen to reach room temperature. It is important for calculation of tempering time. In this case it takes around 1800 seconds or 0.5 hours for it to reach room temperature.

3.4.2 Quenched for 1 second

- **At end of quenching (1 second)**

  Similar to previous case of 1.35 seconds quenching duration, initially most of specimen is austenitized but upon quenching for 1 second martensite layer is formed on the outer surface of the specimen. Percentage of martensite formed depends strictly on the time of quenching, this can be observed by comparing both the results (Figure 20 and Figure 26). One more thing is of importance here, the percentage of pearlite and bainite also depends on the quenching duration. This can also be observed upon comparing results for both quenching durations

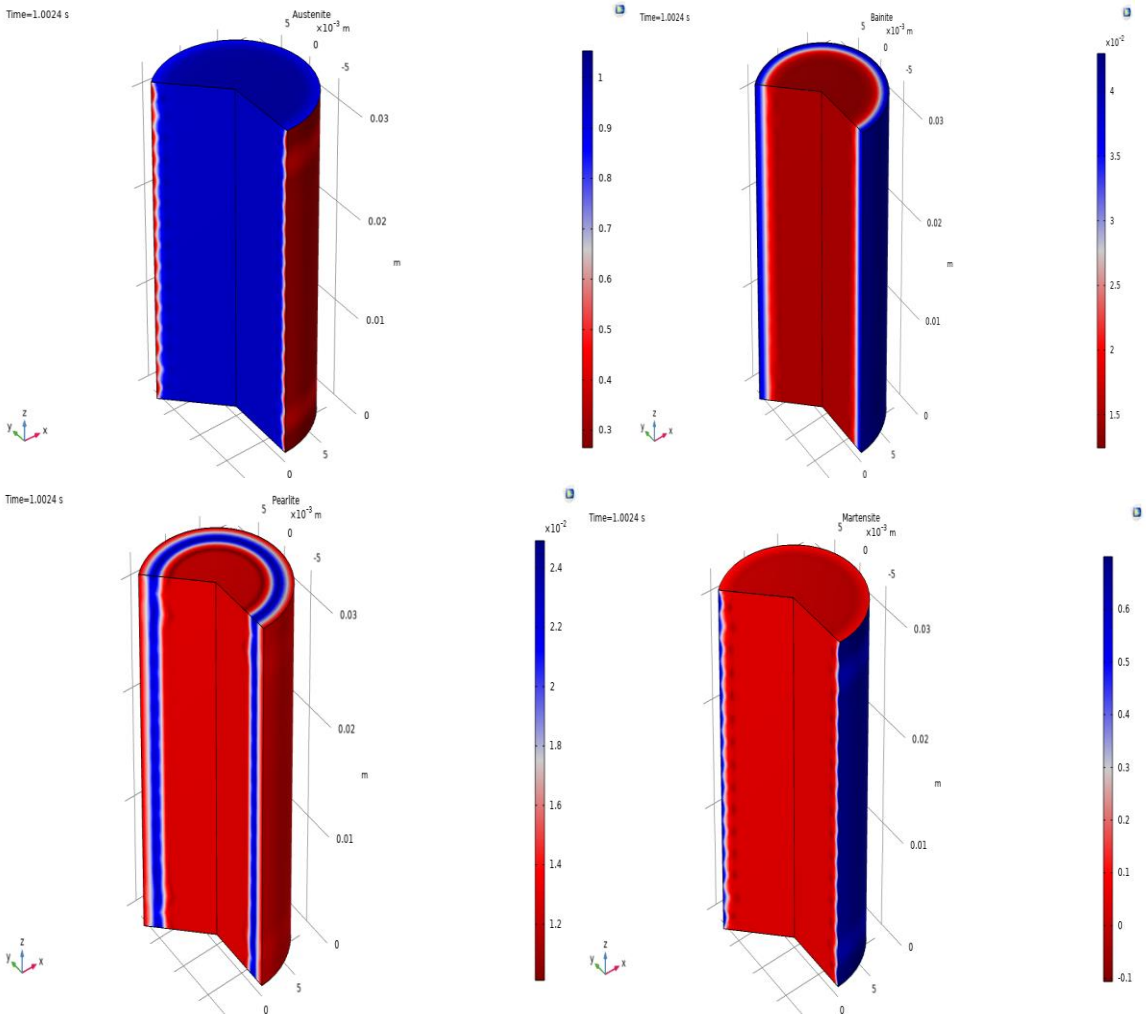

Figure 26 Percentage of all phases at end of 1 second quenching time

- **End of simulation**

The fractions of each phase at the end of simulation are presented in Figure 27. Here surface is covered with martensite and the body is mostly made of pearlite.

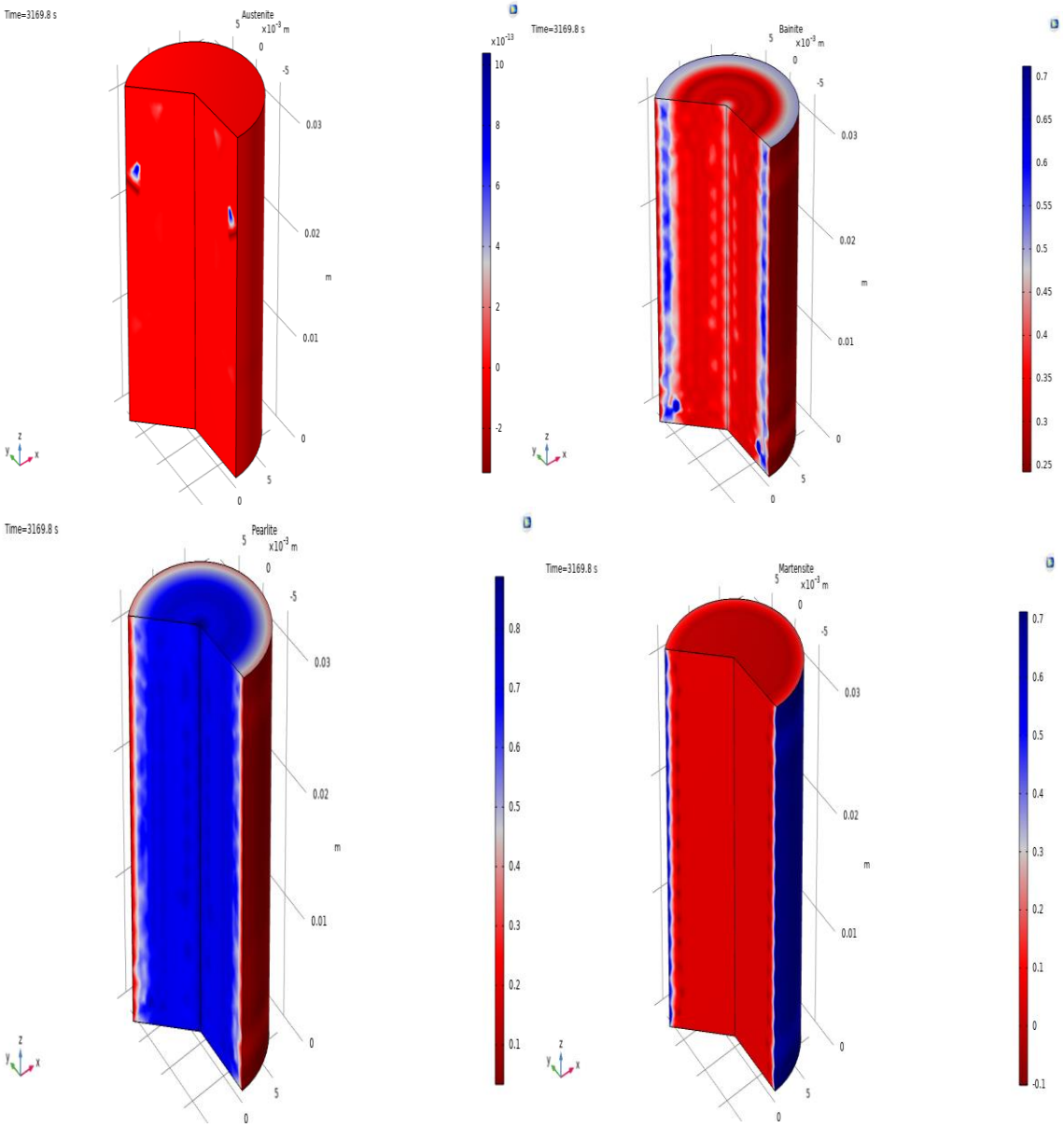

Figure 27 Percentage of all phases at the end of simulation for 1 second quenching experiment

As discussed previously we can see that pearlite is the dominant phase in quenching duration of more than 1.2 seconds.

Martensite as a function of radial distance:

Figure 28 shows phase fraction of martensite as a function of radial distance for 1 second quenching experiment.

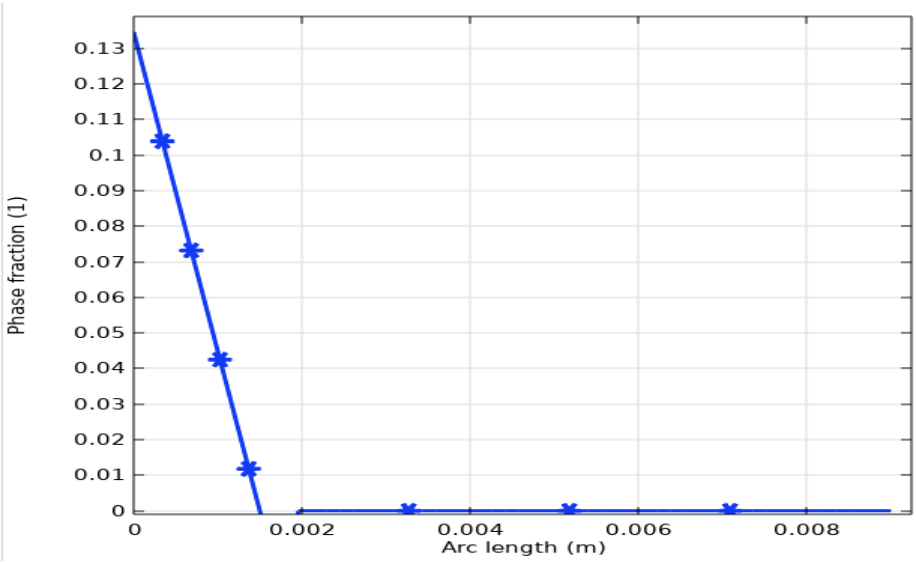

Figure 28 Martensite as a function of radial distance

Phase Fraction of Austenite Pearlite and Bainite against radial distance:

Figure 29 shows phase fraction of Bainite, Pearlite and austenite at the end off simulation.

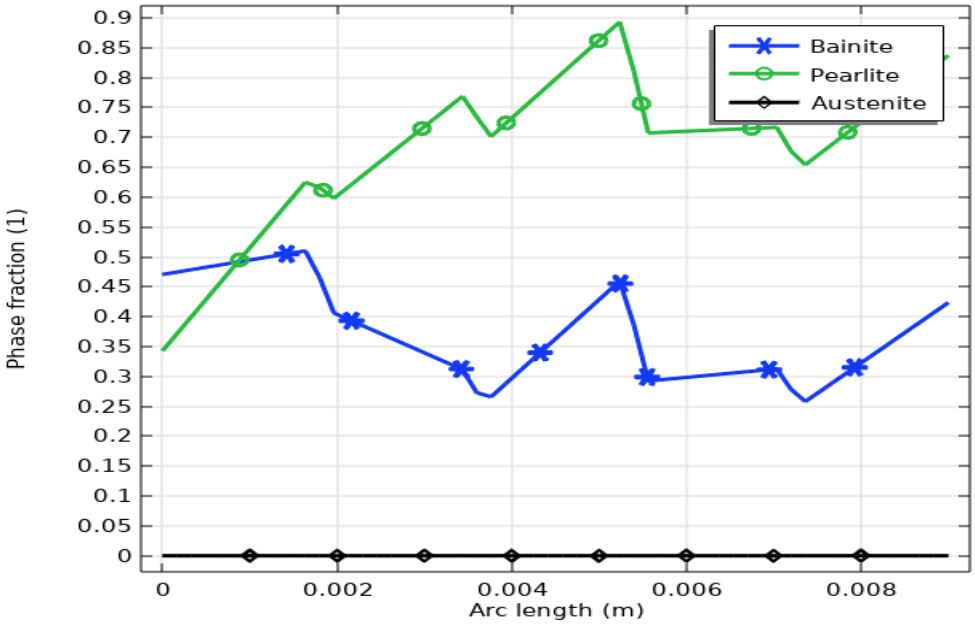

Figure 29 Pearlite, Bainite and Austenite against radial distance

- **Phase fraction of each phase:**

  It can be observed in Figure 30 that the martensite formed in this case is lower that the one for 1.3 seconds quenching time. This was expected as martensite formation depends on quenching time.

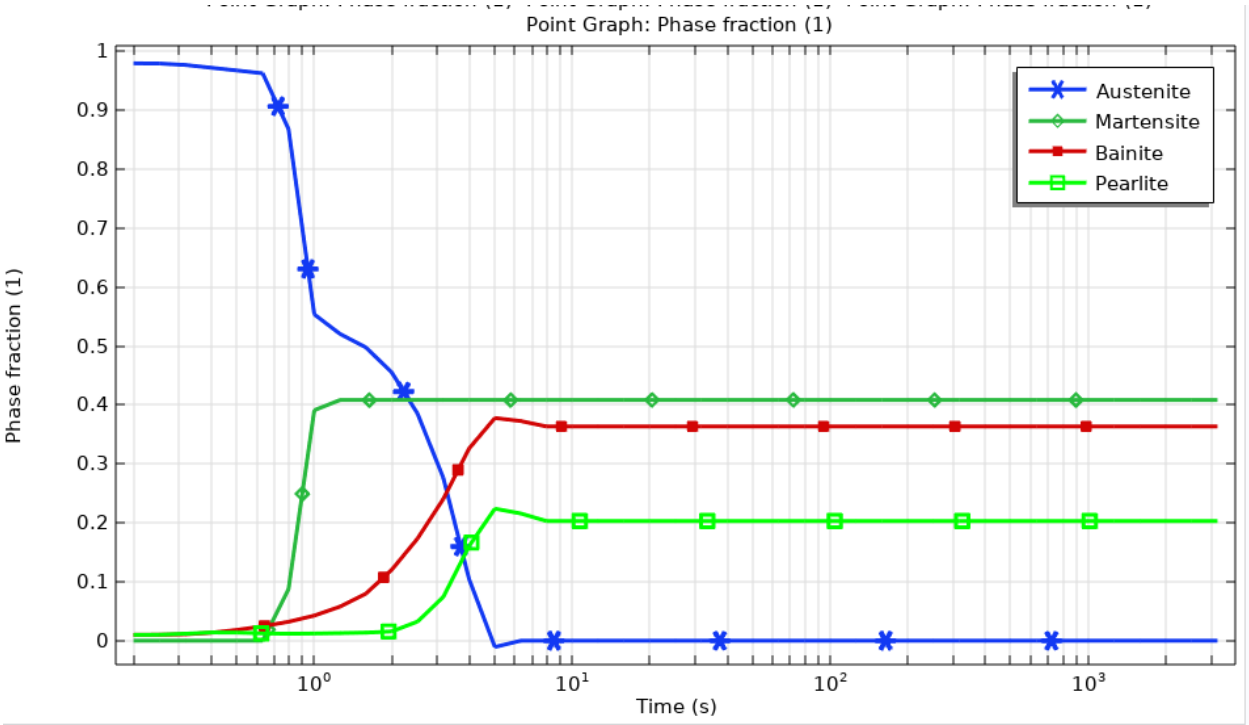

Figure 30 Phase fraction against time for 1 second quenching experiment

- **Temperature of surface and core plotted against time**

  Tempering temperature is almost 620 ℃, it can be read from graph in Figure 31. It is the equilibrium temperature between surface and core.

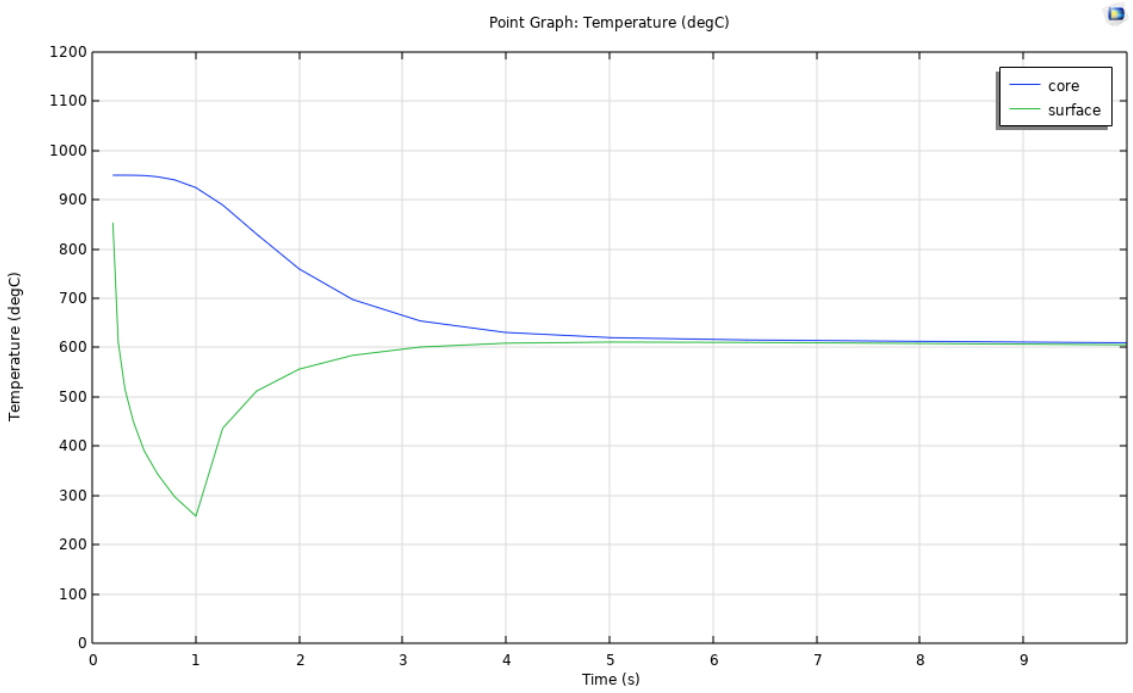

Figure 31 Temperature at Core and Surface against time for 1 second quenching experiment

Tempering time can be calculated by the graph presented in Figure 32 below. In this case it is slightly above 1800 seconds.

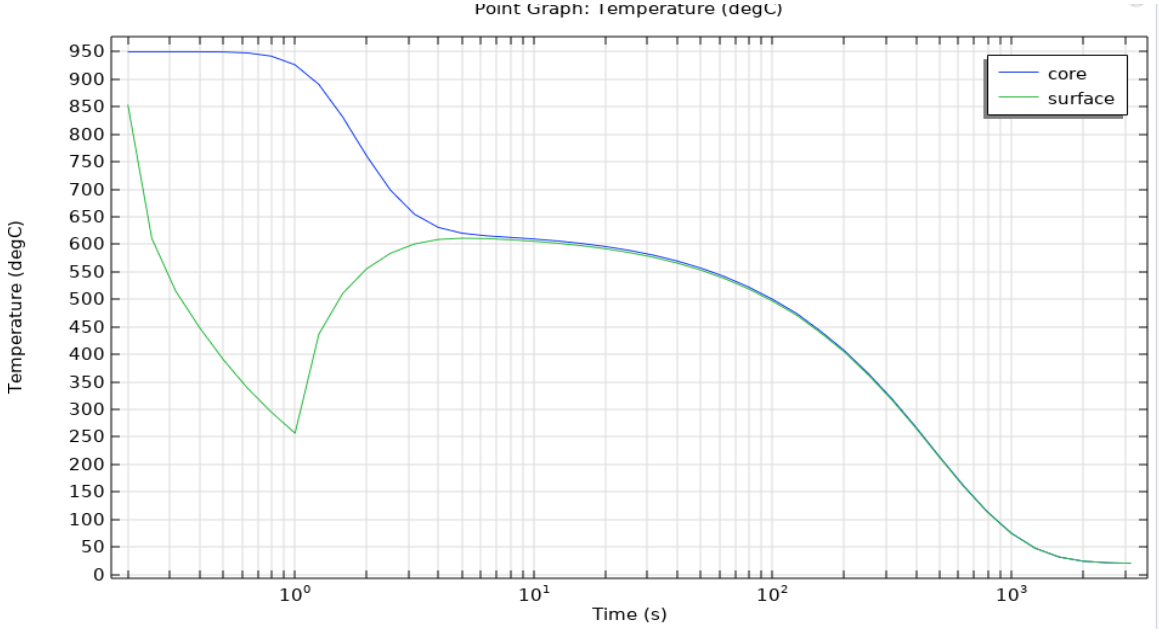

Figure 32 Temperature against time log scale (1 second quenching)

3.5 Comparison with Experimental data

For 18mm bar, experimental and theoretical data is presented by Centinal[5], in their detailed study. Quenching duration is plotted against tempering temperature which is achieved when the temperature of whole specimen becomes equal meaning that the center and surface are at same temperature. The results are superimposed on experimental graph for better understanding presented in Figure 33.

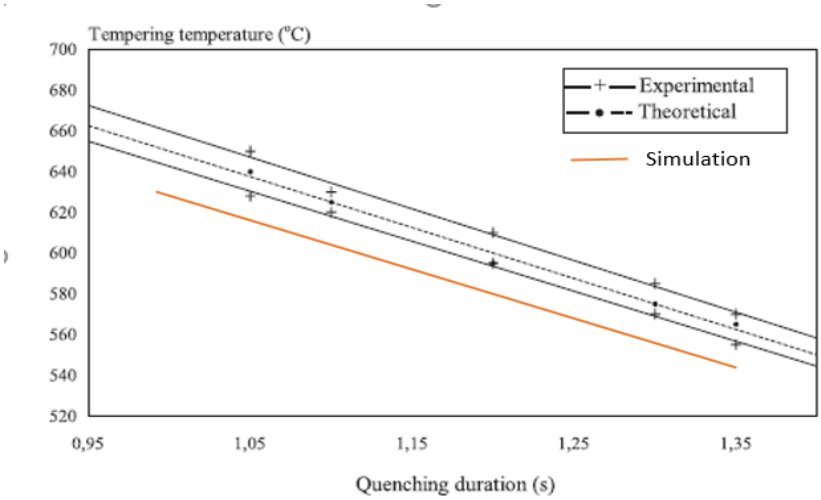

Figure 33 Tempering temperature as a function of quenching time[5] (Simulation results superimposed)

Results are quite promising compared to experimental data and more importantly the values are very close as displayed in the above graph. The simulated values came less than experimental and theoretical ones but still very close.

Figure 34 shows that for quenching time of more than 1.2 seconds approximately bainite is the dominant phase but for less than 1.2 seconds, pearlite is the dominant phase. This proves that our results are in line with experimental data.

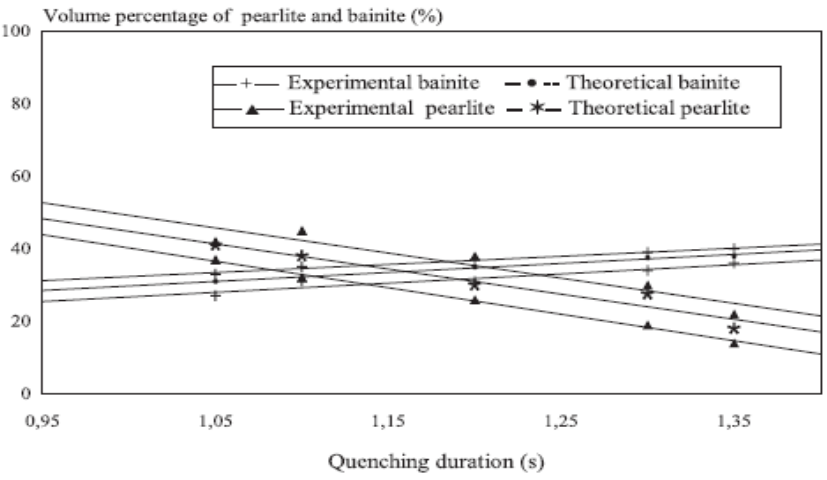

Figure 34 Percentage of Bainite and Pearlite as a function of quenching time (Experimental) [5]

3.6 Martensite Hardness calculation

- **For 1.3 Seconds Quenching**

To calculate hardness of martensite we shall use Hribal, Grange and Porter's[26] method. The first step is to calculate Tempering parameter as in our case tempering is less than 1 hour. Canale[27] wrote that for case of continuous changing temperature same equation can be used as that for isothermal conditions. Following is the equation

$$\mathbf{P = (°F + 460)(18 + \log(t_{hrs})) * 10^{-3}}$$

Tempering time is the time it takes to reach room temperature which in our case is 1800 seconds. So, the parameter value is 26.23. Base hardness of 0.17% carbon steel is 190. Now we add the effect of all elements into this value.

By using the graph provided in literature we can see that 26.3 parameter will produce equivalent effect of 950°F tempered for 1 hour. Since we don't have graphs for 950°F, we will interpolate results between 900°F and 1000°F to get hardness at 950°F.

ΔHV	900°F	1000°F
Si	12	14
Mn	55	45
P	8	8

Table 12 Increase in hardness due to alloying elements after tempering

$$\Delta HV_t = 71$$

$$HV = 251$$

$$HRC = 23$$

Total hardness is achieved by adding base hardness for 0.17% C steel tempered for 1 hour at 950°F and ΔHV due to all alloying elements. Later conversion table was used to convert HV to HRC.

- **For 1 second Quenching**

By using tempering parameter equation presented by Hribal, Porter and Grange, we calculate tempering parameter. Tempering parameter came out to be 28.5, by using graph provided we can find that its value is equivalent to that of steel tempered for 1 hour at 1100°F. Base hardness at 1100°F of 0.17% C steel is almost 155, we add it to the values of hardness increase by each element to get final value. ΔHV due to silicon at 1100°F is approximately 13. ΔHV due to manganese at 1100°F is approximately 49. ΔHV due to phosphorous at 1100°F is approximately 9.So total HV for martensite tempered at 1100°F is 226, which is 17 in HRC.

3.7 Total Hardness calculation

To calculate total hardness of steel we need to calculate the hardness of other phases as well and then apply mixture rule, which is multiply hardness of all the phases with their respective phase fraction and then add all the values. We will use the same method as in section 2.3.3 of Jominy test for hardness calculation of other phases.

For 1.3 seconds quenching time:

We calculate HV index by using the same approach as in 2.3.3, which is firstly calculate cooling rate at 700 ℃ at different radial distances and then using the Ion and Anishdal equations calculate HV index of each phase. Finally apply mixture rule to get final Hardness.

Distance(mm)	f_b . $HV_{bainite}$	f_p . $HV_{pearlite}$	f_m . $HV_{martensite}$	HV
0	0	0	251	251
2	2.9	131.6	0	134.5
4	23.3	108	0	131.3
6	26.2	104.6	0	130.8
8	26.2	104.6	0	130.8

Table 13 Hardness calculation for 1.3 seconds quenching simulation

For 1 second quenching time:

Like previous section HV is calculated for 1 second quenching experiment using same method.

Distance(mm)	f_b . $HV_{bainite}$	f_p . $HV_{pearlite}$	f_m . $HV_{martensite}$	HV
0	55.9	51.3	31.6	139
2	46.5	81	0	127
4	35	94.5	0	129.5
6	35	94.5	0	129.5
8	35	94.5	0	129.5

Table 14Hardness calculation for 1 second quenching experiment

Figure 35 shows the comparison between hardness of both simulations. We can see that the hardness for 1.3 seconds quenching simulation is higher due to more martensite present. While the simulation with 1 second quenching time has less hardness because of less martensite formation.

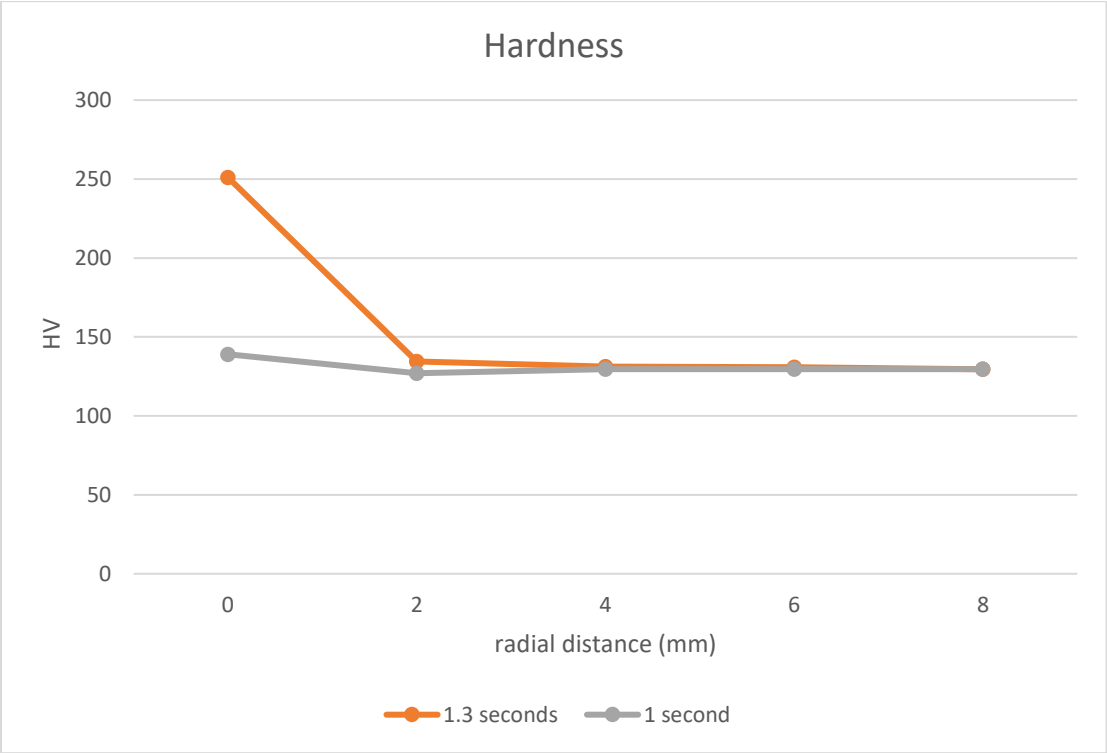

Figure 35 Comparison of hardness after tempering for both quenching simulations

4 Conclusion:

In order to perform our simulation COMSOL Multiphysics was used. This software is quite popular in academic that is the reason to select it so that it is possible to evaluate its use for students in Turin. Two simulations were performed during this thesis, one is Jominy test and the second one is TEMPCORE process. The material used in this thesis is C45 for Jominy, which is medium carbon steel with good mechanical properties and 1020 for Tempcore process which is low carbon steel.

TTT diagram was used to extract experimental data for first simulation. With the help of simplified Avrami law equations values of τ and n were found. For the second simulation value are extracted using equations provided in [5] These values were then put into software using JMAK model to simulate austenite to pearlite and bainite. For austenite to martensite Koistinen-Marburger model was used. Also, to increase the precision of results temperature limits were put into action.

In Jominy test as expected the end of specimen quenched by water was almost 100% martensite with a bit of bainite after that and a lot of Pearlite. The temperature graph at different depths of specimen was plotted against log of time, it was very close to that of provided in the ISO standard for Jominy test. This proves that simulated results very close to those of experimentally obtained values. At the end of simulation, Hardness values were calculated using equations form literature and the results were compared with experimental values and STM standard values using a graph.

In the case of Time Quenching (TEMPCORE process) as soon as the test was initiated, martensite started forming at the surface of specimen and the core was dominantly austenite. This can be seen in 3D plots of specimen showing percentage of different phases at 1.3 seconds in the test. After some time, surface layer was almost completely martensite and other three phases were present in different percentages. The temperature at surface and core of specimen were plotted against log of time. Same process was repeated for 1 second quenching time and results were plotted to better understand the effect of quenching time on tempering temperature and phases present. Hardness values for tempered martensite were calculated using Hribal, Porter and Grange[26] method. Finally total hardness of steel was calculated using the mixture rule and the results were superimposed on a single graph for comparison.

5 References:

[1] Wever, F., Rose, A. and Strassburg, W., 1954. Atlas zur Warmebehandlung der Stahle, Verlag Stahleisen, Dusseldorf.

[2] Matteis, Paolo, Studio degli effetti magneto-termo-metallurgomeccanici indotti da un processo di tempra/distensione ad induzione: analisi sperimentale e validazione numerica con codice F.E.M., Tesi di Laurea, Politecnico di Torino, AA 2000, Debenedetti B., Maizza G.

[3] Numerical Simulation of solid-state metallurgical processes, Bachelor thesis 2020/21 Marcello Galleini, Prof. Matteis Paolo.

[4] Tzitzelkov, I., Hougardy, H.P. and Rose, A., 1974. Mathematische Beschreibung des Zeit-Temperatur-Umwandlung-Schaubildes für isothermische Umwandlung und kontinuierliche Abkühlung. Archiv für das Eisenhüttenwesen, 45(8), pp.525-532.

[5] Çetinel, H., Toparlı, M. and Özsoyeller, L., 2000. A finite element based prediction of the microstructural evolution of steels subjected to the Tempcore process. Mechanics of Materials, 32(6), pp.339-347.

[6] Ion, J.C. and Anisdahl, L.M., 1997. A PC-based system for procedure developement in laser transformation hardening. Journal of materials processing technology, 65(1-3), pp.261-267.

[7] Nunura, C.R., dos Santos, C.A. and Spim, J.A., 2015. Numerical–Experimental correlation of microstructures, cooling rates and mechanical properties of AISI 1045 steel during the Jominy end-quench test. Materials & Design, 76, pp.230-243.

[8] TEST, E.Q.O.J., Standard Test Methods for Determining Hardenability of Steel1.

[9] Li, M.V., Niebuhr, D.V., Meekisho, L.L. and Atteridge, D.G., 1998. A computational model for the prediction of steel hardenability. *Metallurgical and Materials transactions B*, *29*(3), pp.661-672..

[10] Avrami, M., 1940. Kinetics of phase change. II transformation-time relations for random distribution of nuclei. The Journal of chemical physics, 8(2), pp.212-224.

[11] Leblond, J.B. and Devaux, J., 1984. A new kinetic model for anisothermal metallurgical transformations in steels including effect of austenite grain size. Acta Metallurgica, 32(1), pp.137-146.

[12] Koistinen, D.P., 1959. A general equation prescribing the extent of the austenite-martensite transformation in pure iron-carbon alloys and plain carbon steels. acta metallurgica, 7, pp.59-60.

[13] Cahn, J.W., 1956. Transformation kinetics during continuous cooling. Acta Metallurgica, 4(6), pp.572-575.

[14] Lusk, M. and Jou, H.J., 1997. On the rule of additivity in phase transformation kinetics. Metallurgical and Materials Transactions A, 28(2), pp.287-291.

[15] Lee, S.J., Pavlina, E.J. and Van Tyne, C.J., 2010. Kinetics modeling of austenite decomposition for an end-quenched 1045 steel. Materials Science and Engineering: A, 527(13-14), pp.3186-3194.

[16] Kirkaldy, J.S. ed., 1978. Hardenability Concepts with Applications to Steel: Symposium, 1977, Chicago: Proceedings. Metallurgical Society of AIME.

[17] UMEMOTO, M., NISHIOKA, N. and TAMURA, I., 1982. Prediction of hardenability from isothermal transformation diagrams. Transactions of the Iron and Steel Institute of Japan, 22(8), pp.629-636.

[18] Agarwal, P.K. and Brimacombe, J.K., 1981. Mathematical model of heat flow and austenite-pearlite transformation in eutectoid carbon steel rods for wire. Metallurgical Transactions B, 12(1), pp.121-133.

[19] Suehiro, M., Senuma, T., Yada, H. and Sato, K., 1992. Application of mathematical model for predicting microstructural evolution to high carbon steels. ISIJ international, 32(3), pp.433-439.

[20] Lee, J.L. and Bhadeshia, H.K.D.H., 1993. A methodology for the prediction of time-temperature-transformation diagrams. Materials Science and Engineering: A, 171(1-2), pp.223-230.

[21] Han, H.N., Lee, J.K., Kim, H.J. and Jin, Y.S., 2002. A model for deformation, temperature and phase transformation behavior of steels on run-out table in hot strip mill. Journal of Materials Processing Technology, 128(1-3), pp.216-225.

[22] Hömberg, D., 1996. A numerical simulation of the Jominy end-quench test. Acta Materialia, 44(11), pp.4375-4385.

[23] Le Masson, P., Loulou, T., Artioukhine, E., Rogeon, P., Carron, D. and Quemener, J.J., 2002. A numerical study for the estimation of a convection heat transfer coefficient during a metallurgical “Jominy end-quench” test. International Journal of Thermal Sciences, 41(6), pp.517-527.

[24] Trzaska, J., 2016. Empirical formulas for the calculations of the hardness of steels cooled from the austenitizing temperature. Archives of Metallurgy and Materials, 61.

[25] Maynier, P., Jungmann, B. and Dollet, J., 1977. Creusot--Loire system for the prediction of the mechanical properties of low alloy steel products. Hardenability concepts with applications to steel, pp.518-545.

[26] Grange, R.A., Hribal, C.R. and Porter, L.F., 1977. Hardness of tempered martensite in carbon and low-alloy steels. Metallurgical transactions A, 8(11), pp.1775-1785.

[27] Canale, L.C., Yao, X., Gu, J. and Totten, G.E., 2008. A historical overview of steel tempering parameters. International Journal of Microstructure and Materials Properties, 3(4-5), pp.474-525.